

Petrography, Structure, Age, and Thermal History of Granitic Coastal Plain Basement in the Chesapeake Bay Impact Structure, USGS-NASA Langley Core, Hampton, Virginia

By J. Wright Horton, Jr., John N. Aleinikoff, Michael J. Kunk, Charles W. Naeser,
and Nancy D. Naeser

Chapter B of
**Studies of the Chesapeake Bay Impact Structure—
The USGS-NASA Langley Corehole, Hampton, Virginia, and
Related Coreholes and Geophysical Surveys**

Edited by J. Wright Horton, Jr., David S. Powars, and Gregory S. Gohn

Prepared in cooperation with the
Hampton Roads Planning District Commission,
Virginia Department of Environmental Quality, and
National Aeronautics and Space Administration Langley Research Center

Professional Paper 1688

**U.S. Department of the Interior
U.S. Geological Survey**

Contents

Abstract	B1
Introduction	1
Langley Granite (Here Named)	3
Petrography, Mineralogy, and Texture	5
Fractures, Faults, and Veins	8
Neoproterozoic Uranium-Lead (SHRIMP) Zircon Age	9
Thermal History from Argon and Fission-Track Geochronology	10
⁴⁰ Ar/ ³⁹ Ar Analysis of Feldspars	10
Methods	10
Microcline from Granite Sample NL2081	10
Plagioclase from Granite Sample NL2081	15
Albite from Joint-Surface Sample NL2083	16
Fission-Track Analysis of Zircon and Apatite	16
Discussion	20
Regional Comparisons	20
Tectonic Implications for Terranes beneath the Atlantic Coastal Plain	20
Lack of Discernible Impact-Related Deformation or Heating	23
Conclusions	23
Acknowledgments	23
References Cited	23
Appendix B1. Descriptions of Samples from the Langley Granite in the USGS-NASA Langley Core	29

Figures

B1. Regional map showing the location of the Chesapeake Bay impact structure, the USGS-NASA Langley corehole at Hampton, Va., and some other coreholes in southeastern Virginia	B2
B2. Detailed map showing the locations of the USGS-NASA Langley corehole (59E 31) and the 1974 NASA Langley test well (59E 5) at the NASA Langley Research Center, Hampton, Va.	2
B3. Photographs of sections of the USGS-NASA Langley core showing the Langley Granite and its upper contact	4
B4. Photographs of pieces of the USGS-NASA Langley core and photomicrographs of thin sections of the core showing mineralogy, texture, and structure of the Langley Granite	6
B5. Transmitted-light photomicrograph and matching cathodoluminescence image of zircon crystals analyzed to determine a SHRIMP U-Pb zircon age of the Langley Granite in sample NL2081 from the USGS-NASA Langley core	9
B6. Graph showing SHRIMP U-Pb ages of zircon from the Langley Granite in sample NL2081 from the USGS-NASA Langley core	12
B7. Graphs of ⁴⁰ Ar/ ³⁹ Ar age spectra and inverse-isotope-correlation diagrams for three feldspars from samples NL2081 and NL2083 of the Langley Granite from the USGS-NASA Langley core	12

B8.	Graph showing modeled Mesozoic to present-day thermal history of sample NL2081 of the Langley Granite from the USGS-NASA Langley core	18
B9.	Graph showing an example of forward modeling of the estimated long-term thermal history of sample NL2081 (from fig. B8) with a superimposed impact-related thermal “spike” beginning at 35 Ma.	19
B10.	Graph showing a summary of the predicted reduction in apatite fission-track age of sample NL2081 that would result from impact-related heating of varying magnitude and duration	19
B11.	Map showing the location of the USGS-NASA Langley corehole, Hampton, Va., and the Chesapeake Bay impact structure in relation to a tectonostratigraphic terrane map prepared before the structure was recognized.	22

Tables

B1.	Modal composition and rock classification of the Langley Granite from the USGS-NASA Langley core.	B6
B2.	Chemical and normative mineral compositions of two samples of crystalline rocks from the USGS-NASA Langley core.	8
B3.	SHRIMP U-Th-Pb data for zircons from sample NL2081 of the Langley Granite from the USGS-NASA Langley core.	11
B4.	$^{40}\text{Ar}/^{39}\text{Ar}$ age results for three feldspars from samples NL2081 and NL2083 of the Langley Granite from the USGS-NASA Langley core	14
B5.	Apatite and zircon fission-track ages and apatite track lengths for sample NL2081 of the Langley Granite from the USGS-NASA Langley core	17
B6.	Isotopic ages of selected Neoproterozoic igneous rocks for comparison with the age of the Langley Granite	21

Petrography, Structure, Age, and Thermal History of Granitic Coastal Plain Basement in the Chesapeake Bay Impact Structure, USGS-NASA Langley Core, Hampton, Virginia

By J. Wright Horton, Jr.,¹ John N. Aleinikoff,² Michael J. Kunk,² Charles W. Naeser,¹ and Nancy D. Naeser¹

Abstract

The USGS-NASA Langley corehole at Hampton, Va., was drilled in 2000 and was the first corehole to reach coastal plain basement in the late Eocene Chesapeake Bay impact structure. The Langley core provided samples of granite that had been concealed by 626.3 meters (2,054.7 feet) of preimpact, synimpact, and postimpact sediments. The granite, here named the Langley Granite, is pale red, medium grained, massive, and homogeneous in composition and fabric. It has a peraluminous composition (alumina saturation index 1.1) and a seriate-inequigranular, hypidiomorphic, isotropic fabric.

A pervasive secondary mineral assemblage of chlorite + albite + clinozoisite is consistent with either deuteric alteration or lower greenschist-facies metamorphism. Chlorite, the principal mafic mineral, occurs as tabular masses that suggest pseudomorphous replacement of biotite. The top of the granite is weathered but not saproilitized and is nonconformably overlain by Lower Cretaceous clastic sediments.

A SHRIMP ²⁰⁶Pb/²³⁸U weighted average zircon age of 612±10 Ma (2σ) indicates Neoproterozoic crystallization of the Langley Granite. The ⁴⁰Ar/³⁹Ar ages of microcline and plagioclase are consistent with regional cooling and uplift after the late Paleozoic Alleghanian orogeny. Zircon and apatite fission-track cooling ages of 375±44 Ma and 184±32 Ma (2σ), respectively, indicate no discernible impact-related thermal disturbance at the Langley corehole location in the annular trough of the structure about 19 kilometers (12 miles) outside the margin of the central crater.

Modeling the apatite fission-track data places upper limits on the impact-related heating at this location. For an impact-related thermal disturbance equivalent to a modeled thermal spike having a duration of 1 to 0.1 million years, temperatures in this part of the impact structure could not have been higher than about 100°C–120°C.

Most fractures, faults, and veins in the Langley Granite contain lower greenschist-facies minerals and are inferred to predate the impact. No shock-metamorphosed minerals or other features clearly attributable to the impact were found in the granite. Studies of the granite provide a glimpse into the nature of crystalline terranes beneath the Atlantic Coastal Plain and Chesapeake Bay and provide limits on the geographic extent of impact-generated shock and thermal effects.

Introduction

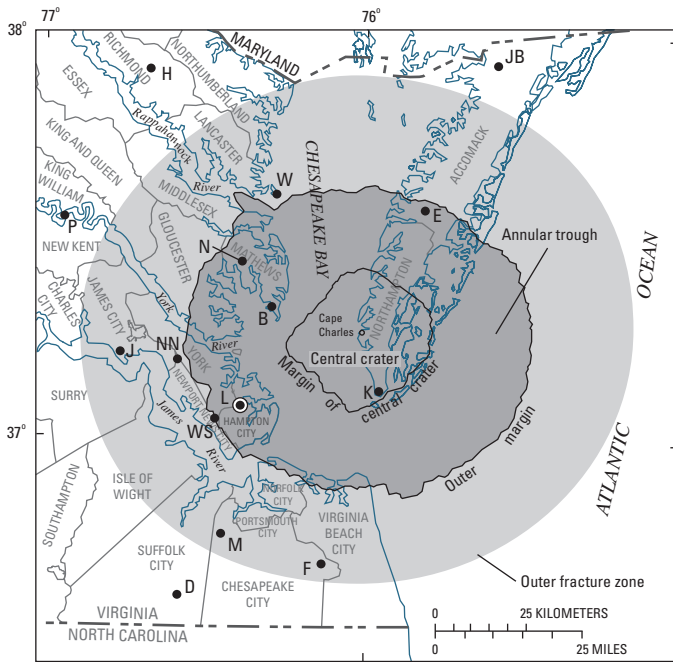
The USGS-NASA Langley corehole at Hampton, Va., was drilled in 2000 and was the first corehole to reach coastal plain basement in the late Eocene Chesapeake Bay impact structure. This structure is near the mouth of Chesapeake Bay, where it lies buried beneath postimpact sediments of the Atlantic Coastal Plain (fig. B1); it was described in earlier reports (Poag and others, 1992, 1994; Poag, 1996, 1997, 1999; Powars and Bruce, 1999; Powars, 2000). The Chesapeake Bay impact structure is one of the largest on Earth and is one of the few fully marine impact structures that have been extensively studied by seismic reflection and drilling (Reimold and others, 2002).

These studies reveal that the buried structure is a complex impact crater 85 kilometers (km; 53 miles (mi)) wide. It consists of an excavated central crater, which is 30–38 km (18–24 mi) wide and 1–2 km (0.6–1.2 mi) deep, surrounded by a flat-floored annular trough, which is 21–31 km (13–19 mi) wide and

¹U.S. Geological Survey, Reston, VA 20192.

²U.S. Geological Survey, Denver, CO 80225.

B2 Studies of the Chesapeake Bay Impact Structure—The USGS-NASA Langley Corehole, Hampton, Va.



- COREHOLES**
- B ● Bayside
 - D ● Dismal Swamp
 - E ● Exmore
 - F ● Fentress
 - H ● Haynesville
 - J ● Jamestown
 - JB ● Jenkins Bridge
 - K ● Kiptopeke
 - L ● USGS-NASA Langley
 - M ● MW4-1
 - N ● North
 - NN ● Newport News Park 2
 - P ● Putneys Mill
 - W ● Windmill Point
 - WS ● Watkins School

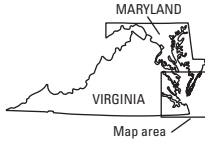


Figure B1. Regional map showing the location of the Chesapeake Bay impact structure, the USGS-NASA Langley corehole at Hampton, Va., and some other coreholes in southeastern Virginia. Locations of the central crater and outer margin are from Powars and Bruce (1999). The extent of the outer fracture zone (light gray) is based on Powars (2000) and Johnson and others (2001); the eastern part is speculative. Illustration modified from Powars, Johnson, and others (2002) and Edwards and Powars (2003).

contains disrupted sediments, a slumped terrace zone, and an eroded escarpment (Poag, 2002; Powars, Gohn, and others, 2002; Powars, Johnson, and others, 2002). This annular trough is encircled by a 35-km-wide (22-mi-wide) outer fracture zone of concentric faults (Powars, Gohn, and others, 2002; Powars, Johnson, and others, 2002).

The innermost part of the annular trough is interpreted by some workers (Poag, Hutchinson, and others, 1999; Poag, 2002; Poag and Norris, this volume, chap. F) to be underlain by a crystalline-rock peak ring that surrounds the central crater. In Poag’s (2002) interpretation, a peak ring was inferred to be about 9 km (5.6 mi) wide and to have about 126 meters (m; 413 feet (ft)) of relief, and the central crater was inferred to contain

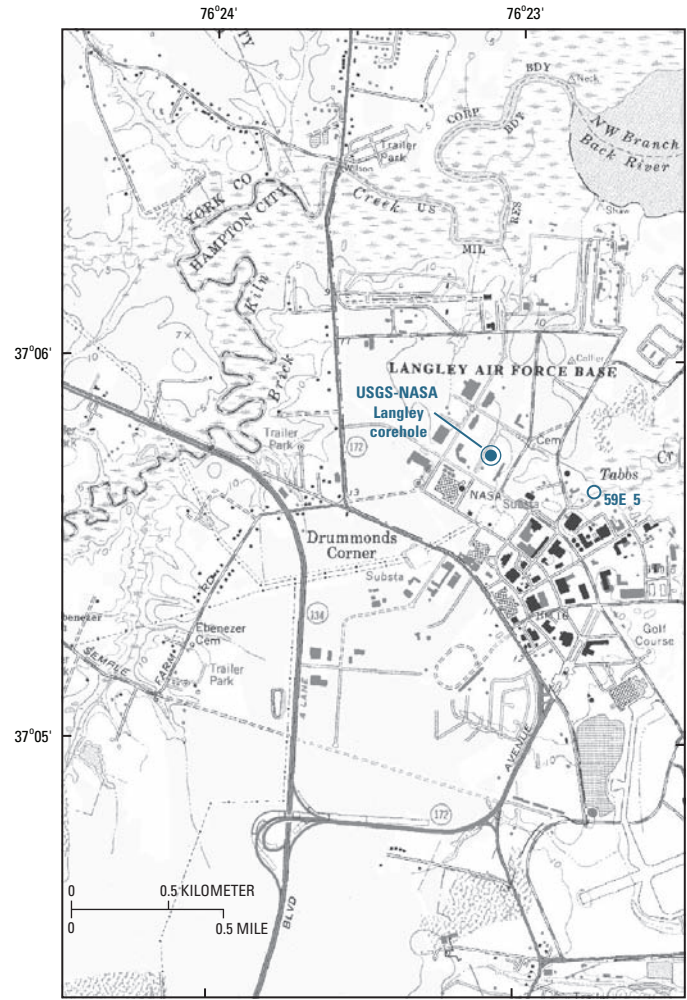


Figure B2. Detailed map showing the locations of the USGS-NASA Langley corehole (59E 31) and the 1974 NASA Langley test well (59E 5) at the NASA Langley Research Center, Hampton, Va. In 2000, the corehole provided samples of granite; for the 1974 well, “granite” was also reported beneath sediments of the coastal plain (Johnson, 1975).

a 5-km-wide (3-mi-wide) central peak having about 620 m (2,034 ft) of relief.

The USGS-NASA Langley corehole is on the York-James Peninsula at the National Aeronautics and Space Administration (NASA) Langley Research Center in Hampton, Va., about 19 km (12 mi) outside the margin of the central crater and about 8 km (5 mi) inside the outer margin of the annular trough as mapped by Powars and Bruce (1999) (figs. B1 and B2). The hole was drilled by the U.S. Geological Survey (USGS) and cooperators (see “Acknowledgments”). Preliminary descriptions of the core are available in Gohn, Clark, and others (2001), Gohn, Powars, and others (2001), Horton and others (2001), and Powars and others (2001).

The core shows a weathered granite below 626.3 m (2,054.7 ft) depth. This granite is overlain by weakly to strongly impact-disturbed preimpact sediments (crater units A and B of Gohn and others, this volume, chap. C), followed by a crater-fill unit informally known as the Exmore beds (Powars and others, 1992; Gohn and others, this volume, chap. C) and by postimpact sediments (Powars and others, this volume, chap. G).

The impact-disturbed sediments include a basal crater unit A, consisting of autochthonous Lower Cretaceous sediments of the Potomac Formation, which Gohn and others (this volume, chap. C) divide into lower beds (nonfluidized) and upper beds (variably fluidized). Crater unit A is present in the Langley core between depths of 626.3 and 442.5 m (2,054.7 and 1,451.7 ft) and is 183.8 m (603.0 ft) thick.

The overlying crater unit B consists of Lower Cretaceous sediments that have zones of extensive fluidization, injection, and mixing (Powars, Gohn, and others, 2002; Gohn, Powars, and others, 2001 and this volume, chap. C). Crater unit B is present in the Langley core between depths of 442.5 and 269.4 m (1,451.7 and 884.0 ft) and is 173.0 m (567.7 ft) thick.

The overlying unit known as the Exmore beds is a polymict diamicton composed of mixed sediments previously interpreted as tsunami deposits (Powars and Bruce, 1999; Powars, 2000) and reinterpreted as mainly seawater-resurge deposits (Gohn and others, this volume, chap. C). The Exmore beds in the Langley core extend from 269.4 to 235.65 m (884.0 to 773.12 ft) depth and have a thickness of 33.8 m (110.9 ft).

Crystalline rocks hidden under the thick blanket of Atlantic Coastal Plain and continental margin sediments make up one of the most poorly understood areas of geology in the United States (LeVan and Pharr, 1963; Denison and others, 1967; Daniels and Leo, 1985; Russell and others, 1985; Pratt and others, 1988; Horton and others, 1991; Rankin, 1994; Glover and others, 1997; Sheridan and others, 1999). Initial results of investigations on crystalline basement and impact-derived clasts from the most recent coreholes in the Chesapeake Bay impact structure were summarized in Horton and others (2001), Horton, Aleinikoff, and others (2002), and Horton, Kunk, and others (2002).

Studies of granite in the USGS-NASA Langley core, presented below, provide insight into the nature of crystalline basement terranes beneath the Atlantic Coastal Plain and Chesapeake Bay. They also provide boundary constraints on the geographic extent of impact-generated shock and thermal effects for numerical models of the late Eocene impact event.

Langley Granite (Here Named)

The Langley Granite is here named for the NASA Langley Research Center in Hampton, Va., where it was recovered in drill core from the USGS-NASA Langley corehole. The corehole site (fig. B2) is designated the type locality. It is “a short

distance north of Langley Boulevard and southwest of Building 1190 in an open grassy area” (Powars and others, 2001, p. 3). The corehole is at lat 37°05'44.28" N., long 76°23'08.96" W. (North American Datum of 1927), at a ground-surface altitude of 2.4 m (7.9 ft) above the North American Vertical Datum of 1988.

Chloritized granite in the core extends from the upper contact at a depth of 626.3 m (2,054.7 ft) to the end of the core at 635.1 m (2,083.8 ft) below the ground surface (fig. B3A). In the corehole, the Langley Granite is overlain by clastic sediments of crater unit A, which are derived from the Cretaceous Potomac Formation; the upper contact of the granite is visible in the core as a sharp nonconformity (figs. B3B and B3C). The uppermost granite is highly weathered and crumbly, but no saprolite is present. Of the 8.9 m (29.1 ft) of granite core recovered, only the lowest ~0.9 m (~3 ft) is mostly unweathered except along fractures. The core shows a weathering profile in granite that appears to have been essentially homogeneous in original composition and grain size. The progressive decrease in weathering with increasing depth below the upper contact is conspicuous.

The top of the coastal plain basement in this area is characterized on seismic-reflection profiles by a distinct pair of reflectors (Catchings and others, this volume, chap. I), which we interpret as the top of the weathered granite (or other crystalline rock) and the base of the underlying transition from weathered to unweathered rock. The thickness of the weathering profile based on these data is about 40 m (about 130 ft).

Rounded pebbles of the granite in overlying Cretaceous sediments are present within about 2 m (6 ft) of the contact in the Langley core (fig. B3B,C); the pebbles diminish upward in size and abundance. The upper contact of the granite in the core is not faulted, although irregularly spaced faults were observed in the Langley core through the overlying Cretaceous sediments.

The areal extent of the Langley Granite beyond the USGS-NASA Langley corehole is undetermined because the body is concealed by coastal plain sediments. The Langley Granite was apparently drilled in 1974 in well 59E 5 (fig. B2), where “granite” cuttings were reported from a depth of about 636 m (2,088 ft) (table 1 of Johnson, 1975); a full description of the rock in these cuttings is unavailable. The location of this well in figure B2 is from unpublished USGS drilling records provided by Gregory S. Gohn (USGS, written commun., 2001) and is consistent with Powars and Bruce (1999, appendix 1A); it is at lat 37°05'38" N., long 76°22'43" W. Both the 59E 5 well and the newer USGS-NASA Langley corehole are located within a poorly defined 28-milligal gravity low, which was interpreted as evidence for a buried granitoid pluton in the vicinity of the NASA Langley Research Center before the Langley corehole was drilled (Daniels and Leo, 1985; Horton and others, 1991).

B4 Studies of the Chesapeake Bay Impact Structure—The USGS-NASA Langley Corehole, Hampton, Va.

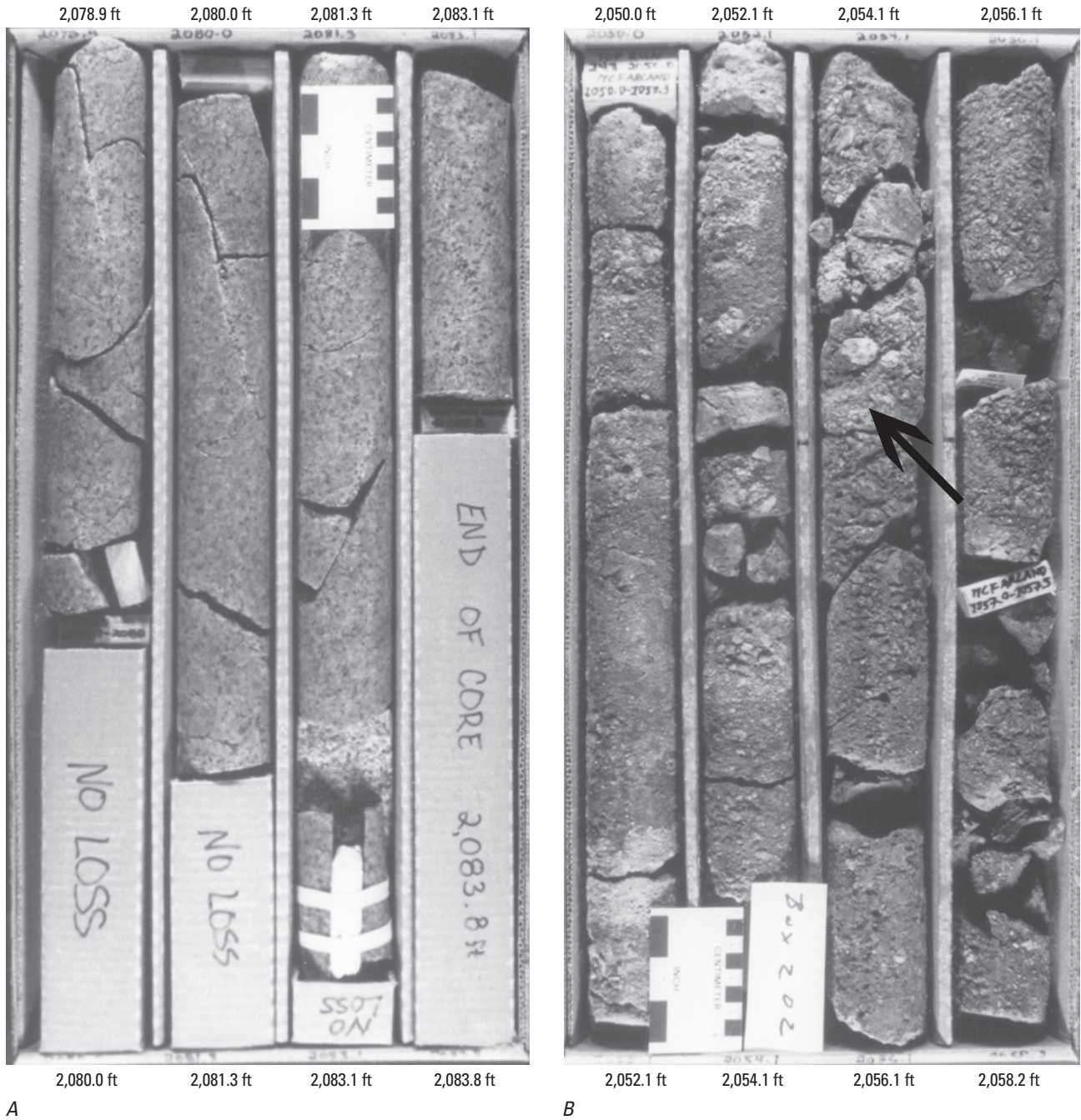
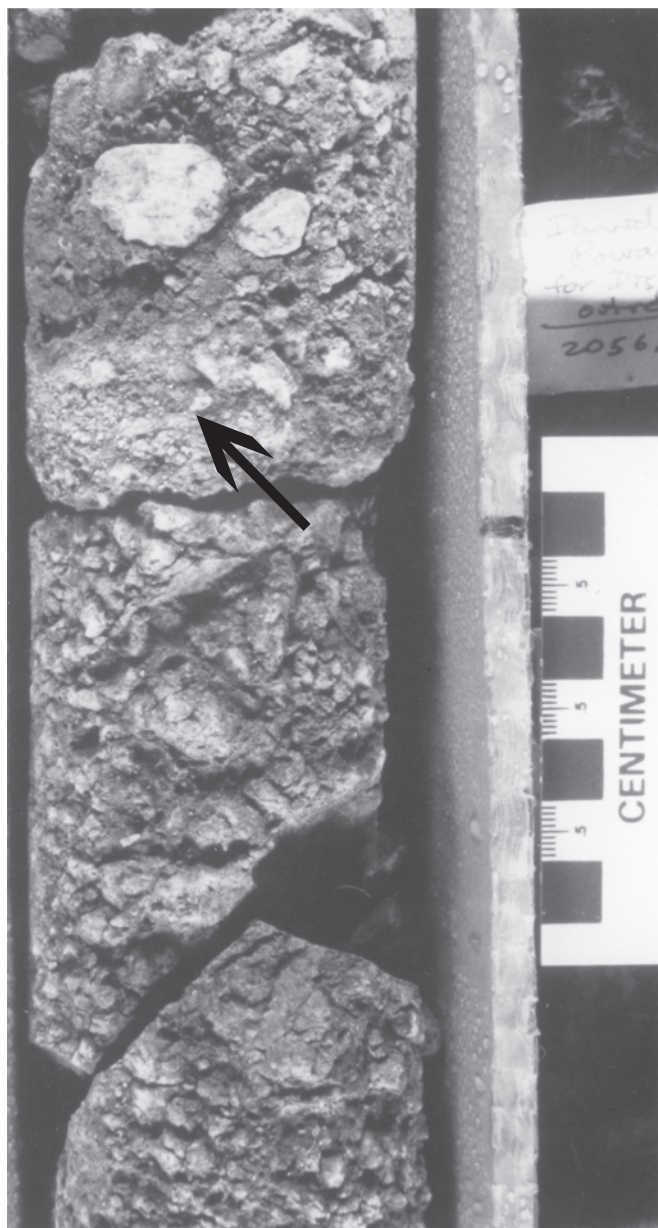


Figure B3. Photographs of sections of the USGS-NASA Langley core showing the Langley Granite and its upper contact. In core boxes, depth increases from left to right and top to bottom. Depths handwritten on the core boxes in feet are repeated in type for clarity. *A*, Core box 206 showing the deepest, least weathered section of Langley Granite core from 633.6 to 635.1 m (2,078.9 to 2,083.8 ft) depth; the granite is massive, medium grained, homogeneous in composition and fabric, nonfoliated, and mostly unweathered except along fractures. White spacer in the third column replaces slab from which sample NL2083.1 was taken. The scales are in centimeters (right side) and inches (left side). *B*, Upper con-

tact of the Langley Granite in core box 202. Arrow points to the nonconformable contact between the weathered Langley Granite and overlying sediments of crater unit A derived from the Cretaceous Potomac Formation; the contact was drilled at 626.3 m (2,054.7 ft) depth. The contact was in the third column from left, 1.5 cm (0.59 in.) above the tick mark on the cardboard divider when the photograph was taken. The scales are in centimeters (right side) and inches (left side). *C*, Same nonconformable contact (at arrow) in closeup view. The centimeter scale has millimeter subdivisions.



C

Figure B3. Continued.

Petrography, Mineralogy, and Texture

The Langley Granite in the USGS-NASA Langley core is pale red, medium grained, massive, homogeneous in composition and fabric, and nonfoliated (fig. B3C; see sample descriptions in appendix B1). The fabric is seriate-inequigranular, hypidiomorphic, homogeneous, and isotropic. The granite consists of oligoclase and albite (33–35 percent by volume), microcline (21–25 percent including perthite), quartz (32–40 percent), greenish-black chlorite (4–8 percent), and less than 1 percent opaque minerals (table B1). The rocks in all four of the thin sections examined are classified as monzogranite. Trace

minerals identified by optical microscope, scanning-electron microscope (SEM), and X-ray diffraction include monazite, clinozoisite, titanite (within chlorite), hematite, iron-titanium oxides, apatite, and zircon. No amphibole, biotite, muscovite, garnet, or cordierite were found.

The microcline is mostly perthitic, having albite intergrowths and clean albite-free rims (fig. B4A). Plagioclase crystals are euhedral to subhedral, have concentric zones accentuated by differences in saussuritization, and locally coalesce as glomerocrysts. Both oligoclase and albite are present. In thin section under transmitted light, the oligoclase and albite appear cloudy, whereas quartz is clear. Quartz commonly has undulatory extinction, and some of the largest crystals have deformation bands. Disseminated micrographic (granophytic) intergrowths of microcline, quartz, and plagioclase make up about 10 percent of the rock. This granophyre, formed by the simultaneous crystallization of feldspars and quartz, is interpreted to represent the last fraction of granite to crystallize from a water-saturated melt.

Chlorite, the principal mafic mineral, occurs as tabular masses (fig. B4B), suggesting pseudomorphous replacement of biotite. The chlorite is magnesium-rich (as indicated by SEM backscatter data) clinoclone (as determined by X-ray diffraction). SEM backscatter imaging indicates that the chlorite has abundant inclusions of other minerals, including albite, an epidote mineral (clinozoisite?), titanite, and a low-titanium iron oxide. Trace amounts of magnetite evident in hand samples are associated with chlorite.

The granite has been pervasively chloritized, as evidenced by the abundant chlorite in shapes suggesting pseudomorphous replacement of biotite and by the apparent absence of igneous biotite or amphibole. The secondary assemblage of chlorite + albite + clinozoisite is consistent with either (1) subsolidus deuteric alteration of igneous minerals by hydrothermal solutions residual from the magma when the granite was still hot and water saturated (autometamorphism) or (2) lower greenschist-facies regional metamorphism. The lack of foliation or other ductile fabrics suggests essentially static conditions during the chloritization. An apparent lack of pegmatite and aplite may not be meaningful because of the limited amount of granite drill core.

Chemical analyses show that concentrations of major and trace elements in a Langley Granite sample are typical of monzogranite (table B2 and Horton and Izett, this volume, chap. E, table E2). The granite is slightly peraluminous, having an alumina saturation index ($A/CNK = Al_2O_3/[CaO+Na_2O+K_2O]$, mol proportion) of 1.1 and corundum in the CIPW norm. The inferred primary mafic and accessory mineral assemblage of biotite (now totally replaced by chlorite), monazite, and iron-titanium oxides is also consistent with peraluminous rocks.

Chemical analyses were also obtained for a rhyolite clast (NL790.9) from the Exmore beds of the Langley core (table B2). This clast, which is interpreted to be impact derived, is slightly peraluminous and is similar in composition to the granite (Horton and others, 2001; Horton and Izett, this volume, chap. E).

B6 Studies of the Chesapeake Bay Impact Structure—The USGS-NASA Langley Corehole, Hampton, Va.

Table B1. Modal composition and rock classification of the Langley Granite from the USGS-NASA Langley core.

[Mineral percentages were estimated visually from thin sections in transmitted light. Plagioclase includes oligoclase + albite, microcline includes perthite, and chlorite has trace-mineral inclusions. The rock classification was based on proportions of quartz (Q), alkali feldspar (A), and plagioclase (P) in the diagram by Streckeisen (1973, 1976). tr, trace amount (less than 1 percent)]

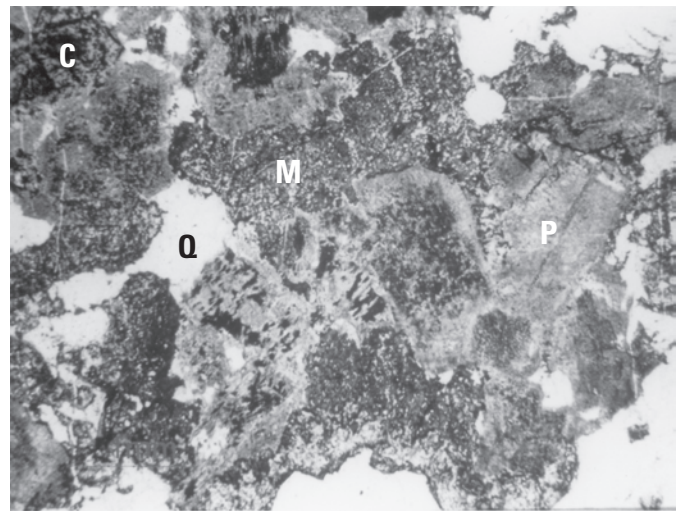
A, Modal composition (volume percent)

Sample no.....	NL2080.1		NL2083.1		Mean	Range
	1	2	1	2		
Thin section.....						
Quartz.....	32	35	36	40	35.75	32–40
Plagioclase.....	35	33	35	35	34.50	33–35
Microcline.....	25	25	25	21	24.00	21–25
Chlorite.....	8	7	4	4	5.75	4–8
Opaque minerals.....	tr	tr	tr	tr	tr	tr
Other minerals.....	tr	tr	tr	tr	tr	tr
Total.....	100	100	100	100	100.00	

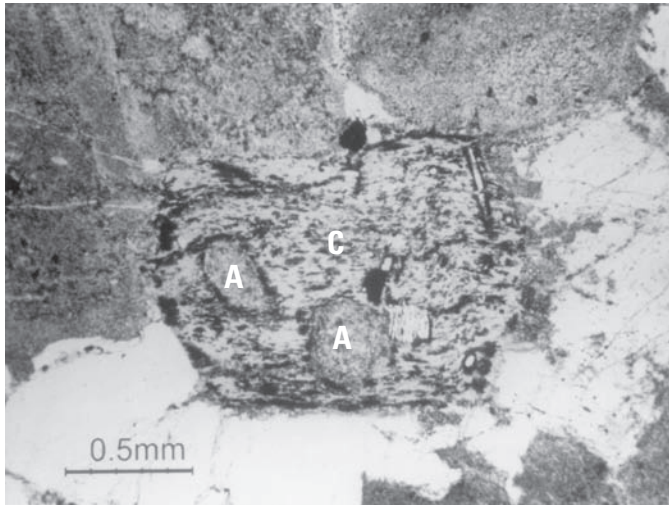
B, Rock classification

Sample no.....	NL2080.1	NL2083.1
Q.....	36	40
A.....	27	24
P.....	37	36
(P/[P+A]) x 100.....	58	60
Name.....	Monzogranite	Monzogranite

Figure B4. Photographs of pieces of the USGS-NASA Langley core and photomicrographs of thin sections of the core showing mineralogy, texture, and structure of the Langley Granite. *A, B, and D* are photomicrographs of thin sections in plane-polarized light; *C, E, F, and G* are photographs of core. *A*, Typical Langley Granite composed of cloudy plagioclase (P) that includes both albite and oligoclase, quartz (Q), perthitic microcline (M) having albite intergrowths and albite-free rims, and chlorite (C) (sample NL2083.1, stained thin section 1, plane-polarized light; vertical dimension is 4 millimeters (mm; 0.16 in.)). *B*, Chlorite (C), in euhedral, tabular shape suggesting pseudomorphous replacement of biotite, contains inclusions of albite (A) and opaque minerals (sample NL2083.1, thin section 2, plane-polarized light). *C*, Joint surface coated by white albite crystals from 633.1 m (2,077.2 ft) depth. *D*, Fracture filled by albite (A) and smaller amounts of chlorite (C) (NL2080.1, thin section 2, plane-polarized light; vertical dimension is 2 mm (0.078 in.)). *E*, Fault surface coated by slickensided chlorite from 631.2 m (2,071.0 ft) depth. *F*, Clinozoisite vein from 631.3 m (2,071.3 ft) depth (see arrow point). *G*, Fracture having open cavities coated by drusy quartz crystals from 631.3 m (2,071.2 ft) depth.



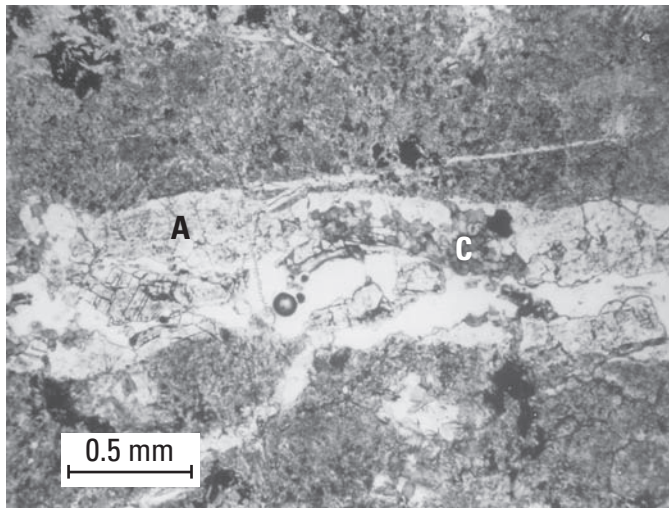
A



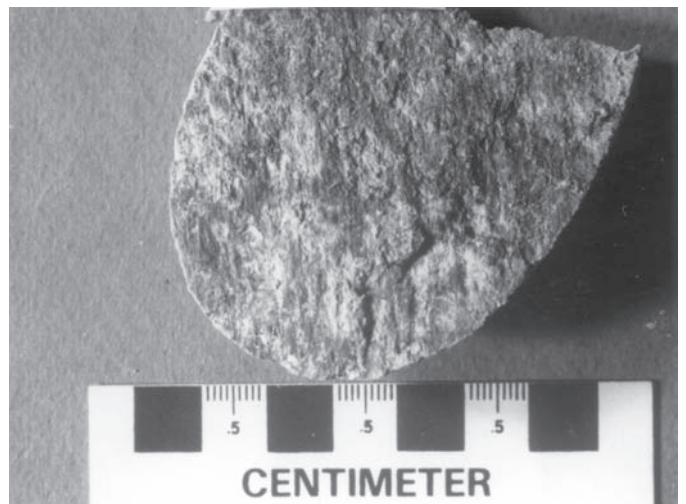
B



C



D



E



F



G

Figure B4. Continued.

Table B2. Chemical and normative mineral compositions of two samples of crystalline rocks from the USGS-NASA Langley core.

[Complete analyses and details are in Horton and Izett (this volume, chap. E)]

Sample no.....	NL2083.1	NL790.9
Rock type.....	monzogranite	rhyolite clast
Unit.....	Langley Granite	Exmore beds
Chemical composition, in weight percent		
SiO ₂	71.0	74.9
Al ₂ O ₃	14.2	12.8
Fe ₂ O ₃	1.90	.83
FeO.....	1.03	.97
MgO.....	.77	.64
CaO.....	1.29	.91
Na ₂ O.....	3.98	4.11
K ₂ O.....	3.48	2.69
H ₂ O+.....	.9	.8
H ₂ O-.....	.1	.1
TiO ₂38	.25
P ₂ O ₅13	.11
MnO.....	.06	.06
CO ₂	<.01	.14
S.....	.42	.18
F.....	.04	.02
Total.....	99.7	99.5
Normative mineral composition (CIPW norms), in weight percent		
Quartz.....	30.98	37.74
Orthoclase.....	20.56	15.90
Albite.....	33.67	34.77
Anorthite.....	5.55	3.80
Hypersthene.....	1.92	2.39
Magnetite.....	2.41	1.20
Ilmenite.....	.72	.47
Hematite.....	.24	.00
Corundum.....	1.85	1.74
Apatite.....	.30	.25
Total.....	98.2	98.26
Oxides for alumina saturation index, in mol percent		
Al ₂ O ₃	9.1	12.6
CaO.....	1.5	1.6
Na ₂ O.....	4.2	6.6
K ₂ O.....	2.4	2.9
A/CNK*.....	1.1	1.1

*The alumina saturation index A/CNK = Al₂O₃/(CaO+Na₂O+K₂O).

Petrologic studies of the chemical and physical parameters that controlled the genesis and evolution of the Langley Granite (including the history of melt production, ascent, and emplacement conditions) and regional geochemical comparisons would require additional rock analyses. Having less than 1 m (3 ft) of granite core that is mostly unweathered is a current limitation.

Fractures, Faults, and Veins

Most of the fractures, faults, and veins in the Langley Granite are coated or filled by chlorite, albite, and clinozoisite, which are typical of lower greenschist-facies metamorphic or similar deuteric alteration conditions, and by quartz. Figure B4C shows a joint surface coated by albite, figure B4D shows a similar fracture filled by albite and smaller amounts of chlorite, figure B4E shows a fault surface coated by chlorite, and figure B4F shows a clinozoisite vein. These fracture-fill minerals probably formed at temperatures higher than the effective closure temperature of about 90°C–100°C for fission tracks in apatite, which yield an age (presented below) far older than the late Eocene impact event. An attempt to directly date albite on a joint surface by the ⁴⁰Ar/³⁹Ar method is described below.

Figure B4G shows a quartz-filled fracture in which open cavities are coated by drusy, comb quartz crystals. Similar dilational fractures are commonly associated with early Mesozoic extensional faults in eastern North America (Garihan and others, 1993). Whether the quartz-filled fractures in the Langley Granite are related to the early Mesozoic continental rifting, earlier deuteric alteration or lower greenschist-facies mineralization, and (or) the late Eocene impact event is undetermined. Fractures in the granite core do not appear unusually abundant in comparison to fractures in drill cores from the Piedmont of the southeastern United States.

The variably mineralized joints in the granite have a wide range of dip angles. Dips were measured for 24 joints (excluding freshly broken surfaces) in the least weathered core section from 633.6 to 635.1 m (2,078.9 to 2,083.8 ft) depth (shown in fig. B3A). Dips for the 24 joints are grouped as follows:

- 8 percent are horizontal to subhorizontal (0°–10° dip)
- 21 percent are gently inclined (11°–30° dip)
- 29 percent are moderately inclined (31°–60° dip)
- 38 percent are steeply inclined (61°–80° dip)
- 4 percent are subvertical to vertical (81°–90° dip)

Faults in the overlying Cretaceous sediments are irregularly spaced in the core, where they are clearly recognizable as planes or planar zones of offset. Although not studied in detail, they include moderately dipping normal faults (identified on the basis of slickensides and rotation of adjacent material) and a few subhorizontal faults, which are visible in the core as local slickensided detachments (J.W. Horton, Jr., unpub. data).

Careful examination of the core revealed no such faults at the upper contact of the weathered granite. There is no evidence from this study of the granite, or from studies of the overlying Cretaceous sediments in the Langley core (Gohn and others, this volume, chap. C), to indicate a major décollement zone just above the granite. Such a zone had been suggested after a preliminary examination of this core (Poag and others, 2001) in order to explain earlier seismic evidence that most normal faults in the overlying sediments do not extend into the crystalline basement (Poag, Plescia, and Molzer, 1999). However, décollements may be found higher in the sedimentary section along the deepest subhorizontal fluidized zone at 558.1 m (1,831.0 ft) depth and in the upper fluidized part of crater unit A (Gohn and others, this volume, chap. C). The seismic-reflection data are more consistent with numerous small-displacement faults than a few large-displacement faults in the preimpact sediments (Catchings and others, this volume, chap. I).

Seismic-reflection data from parts of the Chesapeake Bay impact structure indicate that the top of coastal plain basement is locally offset by high-angle normal faults and low-angle reverse faults, although broad areas of the basement surface appear relatively flat and unfaulted (Poag, Hutchinson, and others, 1999). Catchings and others' (2002) 13.6-km-long (8.5-mile-long) seismic-reflection profile, which is linked to the core samples and to the sonic velocity log from the USGS-NASA Langley corehole, shows nearly 200 m (nearly 650 ft) of relief on the top of basement. Numerous diffractions on the unmigrated profile suggest that inhomogeneities such as the variably mineralized fractures, veins, and faults observed in the granite core are widespread throughout the Langley Granite. Other possible diffractions due to multiple injections, pegmatites, country-rock screens, or xenoliths were not observed in the core but cannot be ruled out because the granite core section is so short. The

seismic profile also shows faults in the overlying sedimentary section, which are interpreted to be related to the late Eocene impact event. A few of these faults are inferred to penetrate and slightly offset the top of the Langley Granite in the general vicinity of the USGS-NASA Langley corehole (Catchings and others, this volume, chap. I). The impact-related faults anticipated from regional seismic-reflection data were not found in the Langley Granite core samples, but the small section (8.9 m or 29.1 ft) of granite core limited the chance of intersecting such faults.

Neoproterozoic Uranium-Lead (SHRIMP) Zircon Age

About 2 kilograms (about 4.4 pounds) of slightly weathered granite from a sawed half of the USGS-NASA Langley core from 633.98 m to 634.81 m (2,080.0 ft to 2,082.7 ft) depth made up sample NL2081; the sample was processed for zircons by standard mineral separation procedures, including crushing, pulverizing, and concentrating heavy minerals by use of a Wilfley table, methylene iodide, and a magnetic separator. Zircons to be dated by sensitive high resolution ion microprobe (SHRIMP) were hand picked, mounted in epoxy, ground to about half-thickness using 1,500-grit wet-dry sandpaper, and polished with 6-micrometer (μm) and 1- μm diamond suspensions. All grains were imaged in cathodoluminescence and were photographed in both transmitted and reflected light prior to SHRIMP measurements to identify pristine areas for analysis and to determine whether components having multiple ages (such as cores and overgrowths) were present (fig. B5).

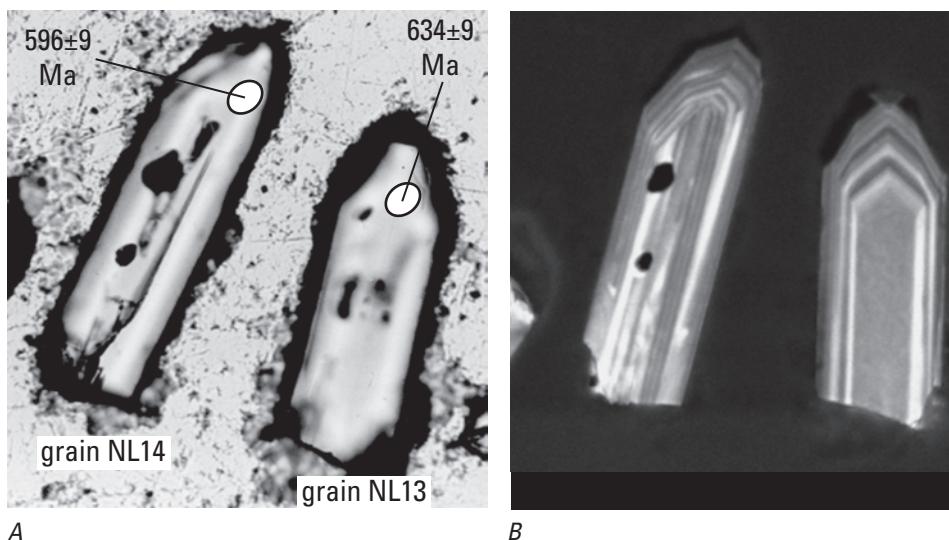


Figure B5. Transmitted-light photomicrograph and matching cathodoluminescence image of zircon crystals analyzed to determine a SHRIMP U-Pb zircon age of the Langley Granite in sample NL2081 from the USGS-NASA Langley core. *A*, Transmitted-light photomicrograph showing external morphology; age data are in table B3. *B*, Matching cathodoluminescence image showing oscillatory internal zones of relatively high (lighter) and low (darker) uranium content. SHRIMP spot diameter is ~ 25 micrometers.

The USGS/Stanford sensitive high resolution ion microprobe-reverse geometry (SHRIMP-RG) at Stanford University was used to date this sample. Analytical procedures followed the methods described in Compston and others (1984) and Williams and Claesson (1987). Zircon standard R33 was used to correct Pb/U ratios for instrumental fractionation. Standard R33 is zircon from monzodiorite of the Braintree Complex, Vermont, that has been dated at 419 Ma (Roland Mundil, Berkeley Geochronology Center, and Sandra L. Kamo, University of Toronto, unpub. data).

Concentrations of U and Th (table B3) are believed to be accurate to about 20 percent. A Tera-Wasserburg plot of ^{204}Pb -corrected isotopic data (plotted as 2σ error ellipses, fig. B6) was used only for visual assessment of the data array to determine which points to include in the age calculation. The age of the sample NL2081 was determined by calculating the weighted average of the $^{206}\text{Pb}/^{238}\text{U}$ ages (using the ^{207}Pb -common Pb correction method of Compston and others, 1984), shown in the figure B6 inset (2σ error bars).

Zircons from the granite are light brown, are euhedral, have length/width ratios of about 3 to 4, and contain fine concentric, oscillatory zoning in cathodoluminescence (fig. B5). A total of 15 grains were analyzed with one analysis per grain. Except in grain NL1, U concentrations are relatively low and have a limited range (129–269 parts per million, ppm) (table B3).

The $^{206}\text{Pb}/^{238}\text{U}$ ages range from 589 ± 9 Ma to 634 ± 9 Ma. The weighted average age from all 15 analyses is 611.6 ± 9.5 Ma (mean square of the weighted deviates (MSWD)=2.5). Excluding five analyses that give ages of 600 Ma or younger results in an age of 621.2 ± 7.6 Ma (MSWD=0.81). However, exclusion of these data based on age alone is subjective and possibly inappropriate. It is possible that these five $^{206}\text{Pb}/^{238}\text{U}$ ages are somewhat low due to a small loss of Pb, but there is no observable evidence in the images of the grains to substantiate this possibility. Thus, the preferred age of igneous zircon, combining isotopic data from all analyzed grains, is rounded to 612 ± 10 Ma (2σ), which is interpreted to indicate a Neoproterozoic crystallization age for the granite.

Thermal History from Argon and Fission-Track Geochronology

Mineral ages that record different closure temperatures collectively provide information on the cooling history of the Langley Granite at the USGS-NASA Langley corehole. Newly determined $^{40}\text{Ar}/^{39}\text{Ar}$ ages of microcline and plagioclase and fission-track ages of zircon and apatite are presented below.

Both the microcline and the plagioclase are altered and have a cloudy appearance in thin section. The alteration is probably to clay or sericite and could be a result of the lower greenschist-facies metamorphism and (or) chemical weathering evident in the core samples.

$^{40}\text{Ar}/^{39}\text{Ar}$ Analysis of Feldspars Methods

Three feldspar separates were dated from the USGS-NASA Langley corehole by using the $^{40}\text{Ar}/^{39}\text{Ar}$ age-spectrum dating technique (fig. B7, table B4). Microcline and plagioclase were separated from the Langley Granite in half the core from 633.98 m to 634.81 m (2,080.0 ft to 2,082.7 ft) depth; this material made up sample NL2081, the same sample from which zircons were also separated, as described above. Albite (sample NL2083) was scraped from a joint surface in the core between 634.81 m and 634.93 m (2,082.7 ft and 2,083.1 ft) depth.

All three mineral concentrates were prepared by using standard techniques, including magnetic separation, density separation, ultrasonic cleaning, and hand picking, to an apparent purity of >99 percent for the microcline and plagioclase and >99.9 percent for the albite. The samples were then re-sieved to remove fine material and were washed in acetone, in alcohol, and three times in deionized water, all in an ultrasonic cleaner.

The $^{40}\text{Ar}/^{39}\text{Ar}$ age-spectrum dating of the three feldspars was done at the U.S. Geological Survey's thermochronology laboratory in Denver, Colo. The samples were packaged in Cu foil capsules and sealed under vacuum into fused silica vials before irradiation in the U.S. Geological Survey's TRIGA reactor (Dalrymple and others, 1981) to convert a portion of their ^{39}K to ^{39}Ar . To monitor this conversion, packets of the standard MMhb-1 hornblende were intercalated with the samples. MMhb-1 has an age of 519.4 ± 2.4 Ma (Alexander and others, 1978; Dalrymple and others, 1981).

The samples dated for this study were analyzed with a VG mm1200b or a MAP 216 mass spectrometer using the $^{40}\text{Ar}/^{39}\text{Ar}$ age-spectrum dating method. Data from procedural blanks were subtracted from the analytical results prior to data reduction. All data reduction for these samples was accomplished by using a modified version of the computer program ArAr* (Haugerud and Kunk, 1988). All estimates of analytical precision are at the 1σ level. Decay constants used are those recommended by Steiger and Jäger (1977). Corrections for the production of interfering reactor-produced argon isotopes from Ca, K, and Cl are those given in Dalrymple and others (1981) and Roddick (1983). Details of the argon analytical technique are in Haugerud and Kunk (1988).

Inverse-isotope-correlation diagrams were prepared by using the method of York (1969). For inverse-isotope-correlation age results to be considered meaningful, we require an MSWD (a goodness-of-fit indicator for the fit of the data to the line) ≤ 2.5 , an initial $^{40}\text{Ar}/^{36}\text{Ar}$ ratio ≥ 295.5 (the ratio in the modern atmosphere), and contiguous regression points.

Microcline from Granite Sample NL2081

Sample NL2081 microcline has the most straightforward results of the three feldspars dated by the $^{40}\text{Ar}/^{39}\text{Ar}$ age-spectrum technique (fig. B7, table B4). The first four steps in the microcline age spectrum (600°C–900°C) decrease in apparent

Table B3. SHRIMP U-Th-Pb data for zircons from sample NL2081 of the Langley Granite from the USGS-NASA Langley core.

[The USGS/Stanford sensitive high resolution ion microprobe-reverse geometry (SHRIMP-RG) at Stanford University was used to date 15 igneous zircon grains (one analysis per grain). Analyst: J.N. Aleinikoff. Analytical procedures are discussed in the text. Definitions of terms: %, percent; ppm, parts per million; Ma, millions of years before present; —, not detected]

Zircon grain analysis	Measured		Common ^{206}Pb (weight %)	U (ppm)	Th/U	Age from			Error, 1 σ (%)	Error, 1 σ (%)	
	$\frac{^{206}\text{Pb}}{^{204}\text{Pb}}$	$\frac{^{207}\text{Pb}}{^{206}\text{Pb}}$				$\frac{^{206}\text{Pb}}{^{238}\text{U}}$ (Ma)	Error, 1 σ (Ma)	$\frac{^{238}\text{U}}{^{206}\text{Pb}}$			$\frac{^{207}\text{Pb}}{^{206}\text{Pb}}$
NL1	2,658.0	0.0627	0.38	741	0.89	589	9	10.49	1.50	0.0572	2.51
NL2	—	.0590	—	176	.75	600	9	10.27	1.54	.0590	2.09
NL3	—	.0624	.28	184	.73	608	9	10.09	1.54	.0624	2.06
NL4	17,872	.0608	.02	269	.98	629	9	9.77	1.49	.0600	1.86
NL5	—	.0615	.17	149	.72	608	10	10.09	1.75	.0615	2.22
NL6	14,415	.0586	—	222	1.14	598	9	10.32	1.51	.0576	1.99
NL7	4,305.1	.0630	.32	155	1.03	619	10	9.93	1.58	.0596	2.96
NL8	—	.0626	.36	230	.93	590	10	10.39	1.81	.0626	1.79
NL9	3,531.7	.0621	.21	160	.95	618	12	9.97	1.92	.0580	2.48
NL10	—	.0615	.12	129	.79	621	11	9.87	1.85	.0615	2.71
NL11	6,138.2	.0600	—	142	.87	619	9	9.95	1.57	.0577	2.88
NL12	—	.0591	—	140	.78	623	10	9.87	1.56	.0591	2.28
NL13	—	.0611	.03	197	.67	634	9	9.68	1.52	.0611	1.91
NL14	10,086	.0616	.22	154	.70	596	9	10.31	1.59	.0602	2.42
NL15	—	.0611	.05	239	.78	629	9	9.74	1.50	.0611	1.74

[†]Radiogenic ratios corrected for common Pb on the basis of the model by Stacey and Kramers (1975).

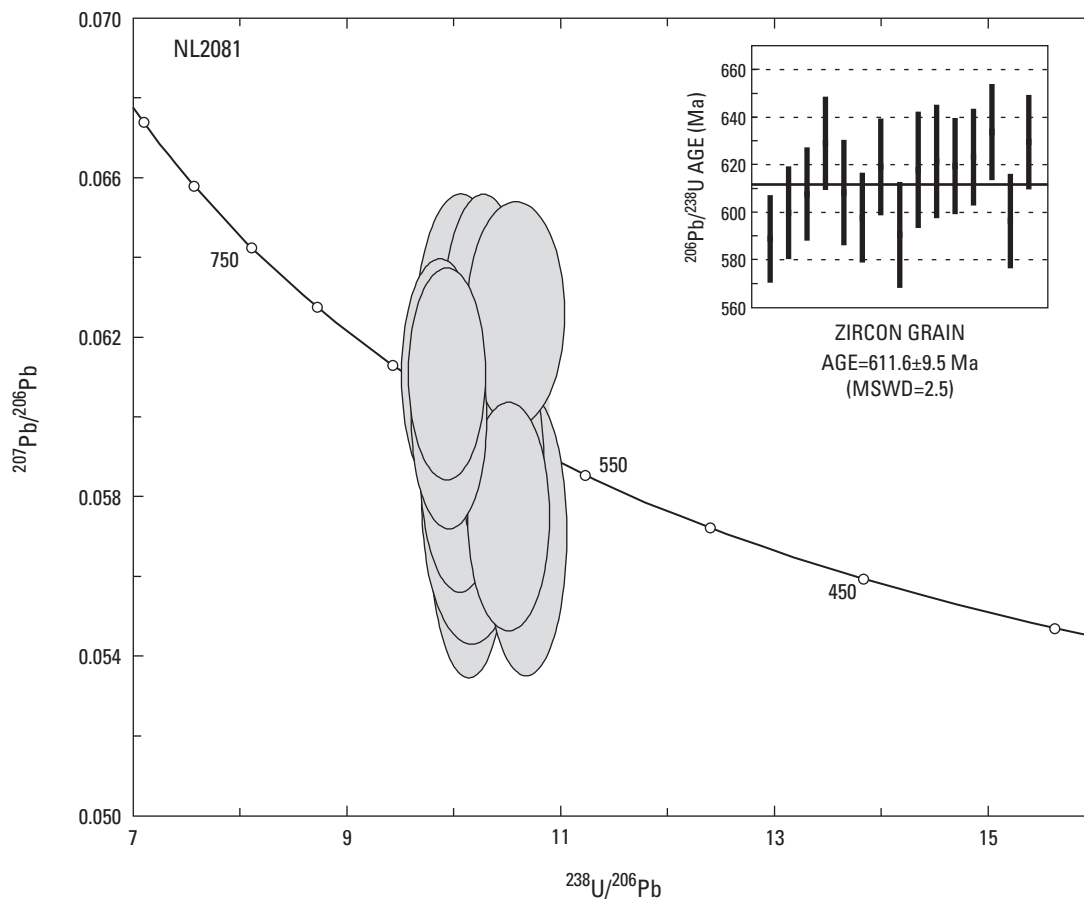


Figure B6. Graph showing SHRIMP U-Pb ages of zircon from the Langley Granite in sample NL2081 from the USGS-NASA Langley core. The main figure is a Tera-Wasserburg concordia diagram with 2σ error ellipses. The inset shows the SHRIMP $^{206}\text{Pb}/^{238}\text{U}$ ages with 2σ error bars. MSWD, mean square of

the weighted deviates. The weighted average age from all 15 analyses is 611.6 ± 9.5 Ma (MSWD=2.5). This age is rounded to 612 ± 10 Ma (2σ) and is interpreted to indicate a Neoproterozoic crystallization age for the Langley Granite. See text for discussion.

Figure B7 (facing page). Graphs of $^{40}\text{Ar}/^{39}\text{Ar}$ age spectra (left) and inverse-isotope-correlation diagrams (right) for three feldspars from samples NL2081 and NL2083 of the Langley Granite from the USGS-NASA Langley core. Data are in table B4. The first step and the last two steps of sample NL2081 plagioclase do not fit in the age-spectra diagram because of the scale used. Height of horizontal boxes indicates 2σ error. For inverse-correlation ages, we require that the mean square of the weighted deviates (MSWD) be ≤ 2.5 , that the initial $^{40}\text{Ar}/^{36}\text{Ar}$ ratio be ≥ 295.5 (the ratio in the modern atmosphere), and that the regressed points be contiguous. Only the regression results presented in the diagrams for microcline and plagioclase meet these criteria. See text for discussion.

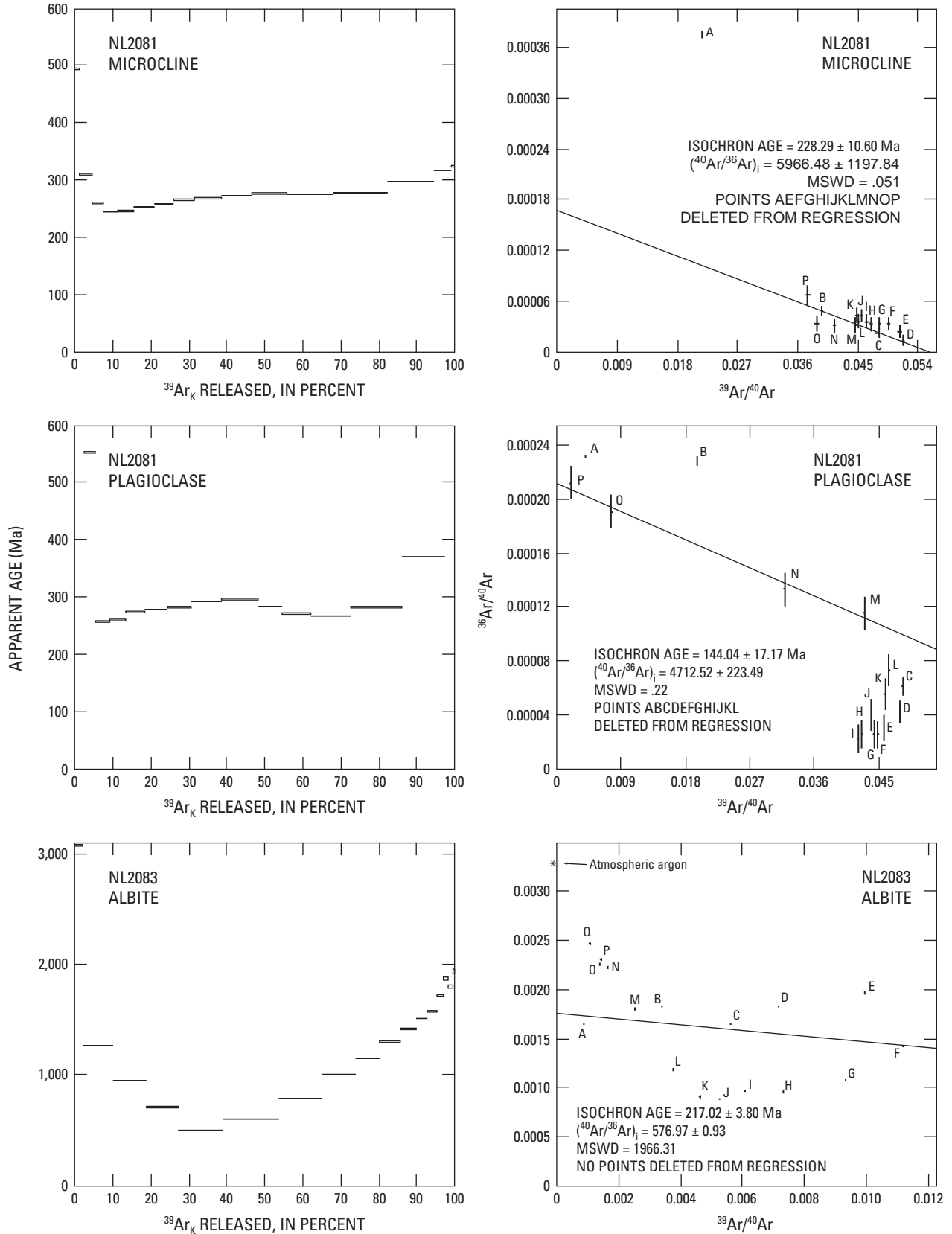


Table B4. $^{40}\text{Ar}/^{39}\text{Ar}$ age results for three feldspars from samples NL2081 and NL2083 of the Langley Granite from the USGS-NASA Langley core.—Continued

Step	Temp (°C)	^{39}Ar (% total)	$^{40}\text{Ar}^*$ (%)	$^{39}\text{Ar}_K$ ($\times 10^{-12}$ mol)	$^{40}\text{Ar}^*/^{39}\text{Ar}_K$	K/Ca	K/Cl	Apparent age (Ma)	Error, $\pm 1\sigma$ (Ma)
Albite from sample NL2083 [0.0094 grams, age spectrum 10KD19, $J=0.007528\pm 0.25\%$]									
A	825	2.0	51.3	0.000572	598.471	0.44	1	3,077.10	2.48
B	950	8.0	46.0	.002243	134.994	.75	3	1,265.03	2.22
C	1,050	8.9	51.2	.002483	91.566	.71	6	945.88	1.41
D	1,150	8.3	45.9	.002317	64.060	.78	10	709.98	1.76
E	1,250	11.9	42.0	.003318	42.101	.95	18	496.66	1.36
F	1,300	14.5	58.2	.004039	52.076	1.11	23	596.69	.98
G	1,320	11.6	68.1	.003243	72.865	.85	20	788.90	.92
H	1,340	8.8	71.9	.002455	98.427	.62	16	1,000.20	1.00
I	1,360	6.3	71.7	.001761	117.923	.51	13	1,146.21	1.26
J	1,380	5.2	73.9	.001455	140.442	.46	11	1,301.35	1.37
K	1,400	4.2	73.2	.001182	158.587	.41	10	1,417.32	1.46
L	1,450	3.2	65.0	.000893	173.499	.39	8	1,507.35	2.02
M	1,500	2.3	46.8	.000632	186.013	.39	5	1,579.58	3.89
N	1,550	1.8	34.3	.000514	210.816	.33	3	1,714.72	4.46
O	1,575	1.3	33.5	.000355	241.463	.28	3	1,868.82	5.42
P	1,600	1.0	32.1	.000281	226.286	.30	3	1,794.15	5.38
Q	1,650	.7	27.0	.000200	255.220	.28	2	1,933.94	7.77
Total gas		100.0	56.9	.027943	108.417	.73	13	1,076.49	
No plateau									

age from 495 Ma to 245 Ma with increasing temperature of release, suggesting the presence of excess argon represented by this part of the age spectrum. The gas represented by the remainder of the age spectrum climbs in apparent age from 245 Ma in the 900°C step to a maximum of 324 Ma in the 1,350°C step. This climbing pattern is almost certainly the result of slow cooling through argon closure in the microcline.

Inverse-isotope-correlation analysis of the age-spectrum data, regressing only points B, C, and D, indicates an apparent age of 228.3 ± 10.6 Ma (1σ). This is not different from the minimum age of 245 Ma in the 900°C step of the age spectrum at the 2σ level of uncertainty. We interpret the maximum age in the age spectrum of 324 Ma to represent cooling through a temperature of about 250°C and the minimum age of 245 Ma to represent cooling through a temperature of about 150°C (McDougall and Harrison, 1999). These ages are consistent with slow cooling following the late Paleozoic Alleghanian metamorphic event. However, it is possible that these ages represent very slow cooling from an earlier Acadian metamorphic event or Alleghanian uplift following Acadian metamorphism.

Plagioclase from Granite Sample NL2081

Sample NL2081 plagioclase has a more complex age spectrum than the microcline has (fig. B7, table B4). The apparent age decreases in the first three steps from 1,849 Ma to 258 Ma, indicating the presence of some excess argon. The apparent ages then increase to 296 Ma in the 1,050°C step, before declining to 266 Ma in the 1,200°C step, and finally climbing to 2,799 Ma in the 1,400°C step. The climb in apparent ages in the high-temperature parts of the age spectrum is again the result of the inclusion of excess argon in the sample. The bulk of the gas was released between the 750°C and 1,250°C steps and has apparent ages ranging from 258 Ma to 296 Ma. Although we do not understand the convex upward shape of the age spectrum in this temperature range, which may be the result of alteration or weathering of the sample, the age results are consistent with those of NL2081 microcline and suggest cooling through closure following the late Paleozoic Alleghanian orogenic event.

Inverse-isotope-correlation analysis of the age-spectrum data from this sample produces an interesting apparent age result. By regressing only the last four steps in the age spectrum

(points M, N, O and P), a very imprecise apparent age of 144 ± 17 Ma can be calculated. Regional palynological data (Doyle and Robbins, 1977; Reinhardt and others, 1980) indicate that the sediments deposited directly on crystalline basement in the vicinity of the Langley corehole are Aptian in age (about 121 to 112 Ma), suggesting that the weathering profile observed in the granite developed in the Aptian or earlier. The apparent age of 144 ± 17 Ma is consistent with that timing for weathering. No other acceptable apparent ages were resolvable from the inverse-isotope-correlation diagram.

Albite from Joint-Surface Sample NL2083

The age spectrum of sample NL2083 albite from a joint surface is dominated by the effects of excess argon (fig. B7, table B4). Apparent ages decrease from 3,077 Ma in the 825°C step to a minimum of 497 Ma in the 1,250°C step and then climb to 1,934 Ma in the 1,650°C step. The age spectrum has a classic U-shape that is indicative of the presence of excess argon.

Inverse-isotope-correlation analysis of the age-spectrum data from this sample does not provide a meaningful age. The pattern of the points in the correlation diagram suggests that the isotopic composition of excess argon could have been changing in the geologic environment of the joint as the albite was crystallizing. We interpret the minimum apparent age in the age spectrum of 497 Ma as the maximum possible age for the formation of this albite. It is important to note that it could have formed hundreds of millions of years after this time.

Fission-Track Analysis of Zircon and Apatite

Fission tracks in a mineral result from spontaneous fission of ^{238}U present in trace amounts in the mineral. The age of a mineral can be calculated from the number of tracks and amount of uranium it contains. However, when a mineral containing fission tracks is heated at a sufficiently high temperature, the tracks shorten and ultimately disappear. The thermal annealing (shortening) of fission tracks and resulting reduction in fission-track age and track lengths provide information on the temperature history of rocks (Naeser, 1979; Gleadow and others, 1986). In a relatively stable geologic environment, apatite undergoes significant annealing between about 60°C and 110°C (Fitzgerald and others, 1995) and has an effective closure temperature (Dodson, 1979) of about 90°C–100°C. Higher temperatures would be required to produce annealing during relatively short-term, impact-related thermal disturbances. The annealing temperatures of zircon are not as well known but are significantly higher than those of apatite; in zircon damaged by natural alpha radiation, the fission-track closure temperature is probably in the range of $\sim 235^\circ\text{C}\pm 25^\circ\text{C}$ (Brandon and others, 1998).

Apatite and zircon were separated from the Langley Granite in sample NL2081 (see appendix B1) of the USGS-NASA Langley core; the sample came from a depth of 633.98 m to

634.81 m (2,080.0 ft to 2,082.7 ft). Separation methods are described above in the section on “Neoproterozoic Uranium-Lead (SHRIMP) Zircon Age.”

Fission-track ages were determined by using the external detector method (Naeser, 1976, 1979; Naeser and others, 1989), as follows. The apatite separate was mounted in epoxy, polished, and etched in 7 percent nitric acid for 40 seconds at 23°C. Zircons were mounted in Teflon, polished, and etched in a eutectic KOH-NaOH melt (Gleadow and others, 1976) for 32 hours at about 214°C. The grain mounts were irradiated with low-uranium-content-muscovite external detectors. Grain mounts and external detectors were counted at $\times 1,250$ magnification using a $\times 100$ oil immersion lens. Ages were calculated by using the zeta calibration method (Hurford and Green, 1982, 1983) (table B5). All fission-track ages are reported at 2σ .

Apatite fission-track lengths were measured in the apatite grain mount in transmitted light at $\times 1,875$ magnification by using a $\times 100$ oil-immersion lens, a digitizing tablet, and a projection tube calibrated against a stage micrometer (1 unit = 0.01 millimeter). Only well-etched horizontal confined tracks in grains with polished surfaces approximately parallel to the crystallographic *c* axis were measured. Reported track lengths (table B5) are actual measurements, not corrected for length-measurement bias (Laslett and others, 1982).

The apatite fission-track age of sample NL2081 is 184 ± 32 Ma (table B5); this age is consistent with the regional pattern of apatite fission-track ages northwest of the Langley corehole that record regional Mesozoic to present-day relatively slow cooling of the Piedmont and spatially related early Mesozoic basins (Roden and Miller, 1991; Hulver, 1997; Naeser and others, 2001). For example, the NL2081 apatite age is statistically indistinguishable (at $\pm 2\sigma$) from, or older than, apatite fission-track ages determined for exposed to shallowly buried (< 1 km or < 0.6 mi) Proterozoic and Paleozoic metamorphic and igneous rocks and Triassic sedimentary and igneous rocks in the Potomac River area of northern Virginia, Maryland, and the District of Columbia (Naeser and others, 2001) and the Taylorsville basin-Richmond basin area of east-central Virginia (Roden and Miller, 1991). The similarity of the apatite fission-track age for the Langley Granite in the Langley corehole to regional apatite fission-track ages suggests that there was little, if any, impact-related apatite annealing in NL2081.

The mean fission-track length in apatite from sample NL2081 is 13.84 ± 0.59 μm at $\pm 1\sigma$ and is generally statistically indistinguishable from, or somewhat longer than, reported track lengths from Piedmont and early Mesozoic basin rocks in the area (Roden and Miller, 1991; Hulver, 1997; C.W. Naeser and N.D. Naeser, unpub. data); the length data are consistent with relatively slow, undisturbed cooling of the rocks (Gleadow and others, 1986). However, the length data for apatite from sample NL2081 should be considered very preliminary. The low yield of apatite and low spontaneous track density (related to a uranium content of only ~ 3 ppm) resulted in an inadequate number

Table B5. Apatite and zircon fission-track ages and apatite track lengths for sample NL2081 of the Langley Granite from the USGS-NASA Langley core.

[Analysts: C.W. Naeser and N.D. Naeser. Definitions of terms: Lab. no., laboratory number; tr/cm², tracks per square centimeter; %, percent; Ma, millions of years before present; μm, micrometer; —, not determined]

Lab. no. DF	Mineral	No. of grains counted	ρ_s^* x10 ⁶ (tr/cm ²)	No. of tracks counted	ρ_i^{**} x10 ⁶ (tr/cm ²)	No. of tracks counted	ρ_d^{***} x10 ⁵ (tr/cm ²)	No. of tracks counted	$P(\chi^2)^{\dagger}$ (%)	Age ^{††} (Ma±2σ)	Mean track length (μm±σ)	No. of tracks measured	Standard deviation of the track-length distribution ^{†††} (μm)
6895	Apatite	10	0.375	245	1.04	340	0.482	2,930	P	184±32	13.84±0.59	6	1.44
6899	Zircon	9	20.1	1,980	7.88	388	4.73	3,450	P	375±44	—	—	—

* ρ_s , spontaneous track density in tracks per square centimeter (tr/cm²) in the sample for the number of tracks counted; see next column.

** ρ_i , induced track density (reported induced track density = 2 x measured value).

*** ρ_d , track density in muscovite detector covering National Institutes of Standards and Technology (NIST) standard glass SRM 963 (for apatite) or standard glass SRM 962 (for zircon) (Carpenter and Reimer, 1974).

† $P(\chi^2)$, measure of probability that all individual grains counted in a sample are from a single age population; P (“pass”) indicates $P(\chi^2)$ values >5%, F (“fail”) indicates $P(\chi^2)$ values <5%; $P(\chi^2)$ values <5% are generally taken as an indication of a real spread in single-grain ages (Galbraith, 1981; Green and others, 1989).

††Age calculated from the fission-track age equation of Hurford and Green (1982, 1983) by using the sums of the spontaneous and induced track counts obtained for all grains counted in the sample and the following values: $\lambda_D = 1.551 \times 10^{-10}$ /year, $g = 0.5$, $\zeta = 10.752$ for apatite (based on SRM 963) and 319.6 for zircon (based on SRM 962).

†††Standard deviation calculated by combining Poisson errors on spontaneous and induced counts and on counts in detector covering glass standard NIST SRM 963 or SRM 962 (McGee and others, 1985).

of track-length measurements for thermal-history modeling or other quantitative track-length analysis.

The fission-track age of zircon from sample NL2081 is 375 ± 44 Ma. As would be predicted from the apatite age data, there is no indication of impact-related annealing in zircon. The few zircon fission-track ages that have been determined from eastern Piedmont and early Mesozoic basin rocks in Virginia, Maryland, and the District of Columbia (Roden and Miller, 1991; Kohn and others, 1993; Naeser and others, 2001) are all statistically younger than the NL2081 zircon fission-track age.

An anomalous feature of the $^{40}\text{Ar}/^{39}\text{Ar}$ and fission-track data remains unexplained. Zircon fission tracks and argon in potassium feldspar have similar closure temperatures and, thus, typically yield similar cooling ages. However, the $^{40}\text{Ar}/^{39}\text{Ar}$ age of potassium feldspar (microcline) from sample NL2081 (324 Ma maximum age; see above section “Microcline from Granite Sample NL2081”) is significantly younger than the zircon fission-track age, possibly because of the presence of alteration products within the microcline.

In summary, the fission-track data for the granite from about 634.3 m (2,081 ft) depth in the Langley corehole indicate that at 19 km (12 mi) from the margin of the central crater, the impact-related thermal disturbance was not sufficient to cause detectable annealing of fission tracks in zircon or apatite.

The lack of annealing in apatite from sample NL2081 can be used to set an upper limit on the impact-related thermal disturbance at this location in the crater; the limit is based on the maximum temperature that could have been attained without affecting the apatite fission-track age. A preliminary estimate of the maximum temperature was obtained by the following steps. First, the thermal history of NL2081 was modeled for regional cooling with the assumption of no impact-related heating (fig. B8). As noted above, the long-term cooling history of NL2081 cannot be modeled directly because of the low number of measurable apatite track lengths, but for the purpose of this exercise, it was approximated by using track-length data imported from another Piedmont “basement” sample that yielded apatite age and track-length data statistically indistinguishable from data for sample NL2081 (C.W. Naeser and N.D. Naeser, unpub. data). Next, forward modeling was used to predict the reduction in apatite fission-track age that would result from impact-related heating, modeled as the simplest case of a thermal spike of varying maximum temperature and duration superimposed at 35 Ma (time of impact) on the long-term cooling history (fig. B9).

Figure B10 summarizes the predicted reduction in apatite fission-track age that would result from including a thermal spike of 0.1–1 million year (m.y.) total duration and 60°C – 140°C maximum temperature in the time-temperature history of

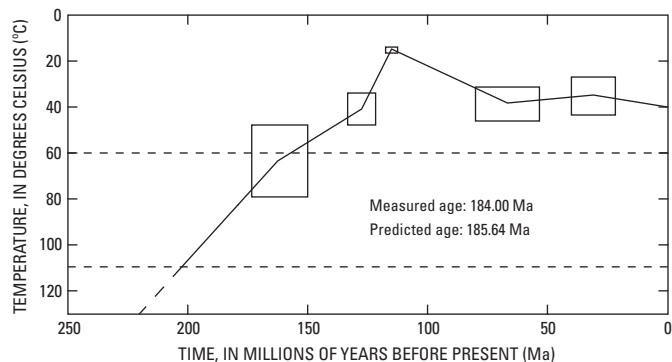


Figure B8. Graph showing modeled Mesozoic to present-day thermal history of sample NL2081 of the Langley Granite from the USGS-NASA Langley core. The plotted curve is the average of a family of thermal-history curves, each of which predicts a statistical match with the measured apatite fission-track age and track-length data. Boxes shown on the plotted curve are $\pm 1\sigma$ bounds on the average time-temperature points that were calculated by the computer model. The dashed horizontal lines at 60°C and 110°C mark the boundaries of the apatite partial-annealing zone in a relatively stable geologic environment. The model was generated by using Kerry Gallagher’s (1995; written commun., 1996) genetic algorithm time-temperature modeling program, Laslett and others’ (1987) annealing model for Durango apatite (from Cerro de Mercado, Durango, Mexico), the measured apatite fission-track age of NL2081, and apatite track-length data from a Piedmont sample with statistically indistinguishable age and mean track length (C.W. Naeser and N.D. Naeser, unpub. data; see text). An annealing model based on Durango apatite is considered appropriate because the mean pit widths of apatite tracks in the analyzed samples indicate an annealing susceptibility comparable to that of Durango apatite. The time-temperature model was constrained to allow NL2081 to be in near-surface conditions in the Aptian (about 121–112 Ma), when deposition of overlying Potomac Formation sediments probably began in this area. This age is poorly constrained in the Langley core (Frederiksen and others, this volume, chap. D) and is inferred from regional information (Doyle and Robbins, 1977; Reinhardt and others, 1980).

NL2081. The plot indicates that for an impact-related thermal disturbance with an effective heating time equivalent to the modeled 1-m.y. thermal spike, temperatures in this part of the crater could not have been higher than about 100°C without producing a significant (at 1σ) reduction in apatite fission-track age. If the thermal disturbance was equivalent to the 0.1-m.y. thermal spike, temperatures as high as about 120°C are possible.

With data from additional coreholes, it may be possible to refine these preliminary estimates of the impact-related thermal structure in the crater.

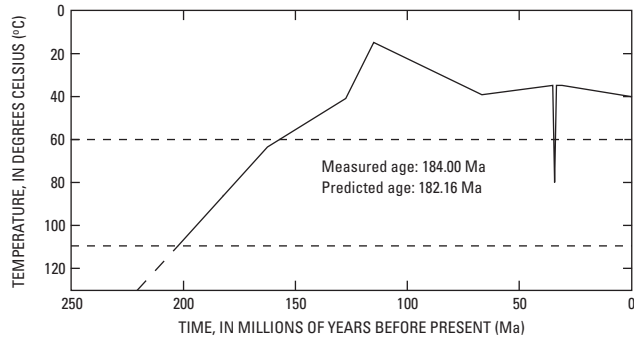


Figure B9. Graph showing an example of forward modeling (by using the program by Kerry Gallagher, 1995; written commun., 1996) of the estimated long-term thermal history of sample NL2081 (from fig. B8) with a superimposed impact-related thermal “spike” beginning at 35 Ma and, in this example, lasting 1 m.y. with a maximum temperature of 80°C. The resulting predicted apatite fission-track age (182.2 Ma) is statistically indistinguishable (at $\pm 1\sigma$) from the measured age of NL2081 (184 \pm 16 Ma), suggesting that an impact-related temperature increase of this magnitude in the part of the crater near the Langley corehole would not have produced a significant reduction in fission-track age.

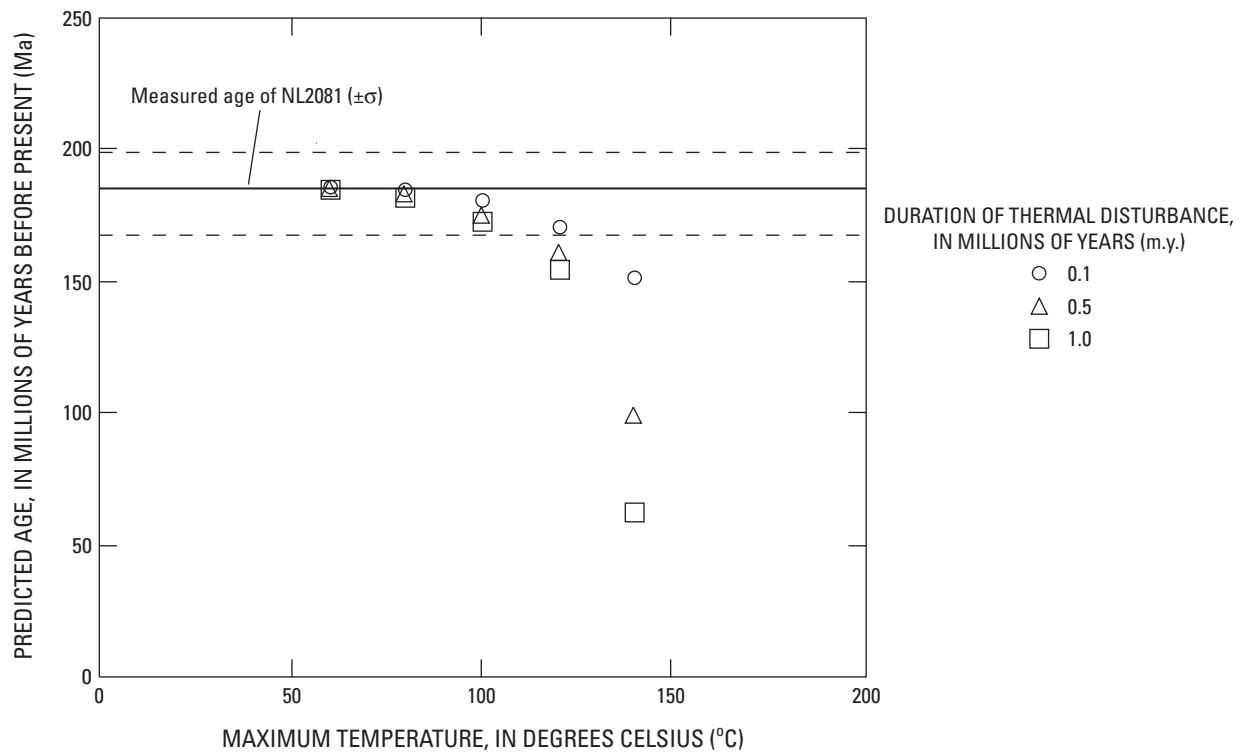


Figure B10. Graph showing a summary of the predicted reduction in apatite fission-track age of sample NL2081 that would result from impact-related heating of varying magnitude and duration (see fig. B9). Horizontal solid and dashed lines indicate the measured age ($\pm 1\sigma$) of NL2081 (184 \pm 16 Ma). The plot suggests that, as a first approximation,

temperatures in excess of 100°C would be required to produce a significant (at 1σ) decrease in age for effective heating times equivalent to a thermal spike of 1-m.y. duration beginning at 35 Ma. For heating times of ≤ 0.1 m.y., temperatures greater than 120°C would be required.

Discussion

Regional Comparisons

Crystalline rocks beneath the Atlantic Coastal Plain in the vicinity of Chesapeake Bay are poorly known, and so a comparison of the Langley Granite with other rocks in the region may help to constrain regional correlations and tectonic interpretations. The Langley Granite differs in age from Neoproterozoic igneous rocks associated with Laurentia (ancestral North America), such as the Crossnore Plutonic Suite (Su and others, 1994; Fetter and Goldberg, 1995) or Catoctin Formation (Aleinikoff and others, 1995). However, igneous rocks of similar age (table B6) are found in magmatic-arc terranes of the Appalachian Piedmont and beneath the Atlantic Coastal Plain of the eastern United States.

Figure B11 shows the position of the Langley corehole and the Chesapeake Bay impact structure on a tectonostratigraphic map (Horton and others, 1991) that was prepared before the structure was recognized. The Langley Granite is similar in age to some of the older igneous rocks in the Carolina, Spring Hope, and Roanoke Rapids terranes of the Appalachian Piedmont, and in the Hatteras terrane beneath the Atlantic Coastal Plain (table B6, fig. B11), and it is comparable in appearance to some of the plutonic rocks. For example, granite in the central part of the Chapel Hill pluton in the Carolina terrane also has micrographic feldspar-quartz intergrowths and chloritization accompanied by an apparent lack of foliation (Mann and others, 1965). Geochemical studies indicate that most of these igneous rocks were derived from magmas generated in a subduction zone, although cordierite-bearing granite at Stumpy Point, N.C., in the Hatteras terrane appears to be an exception (Speer, 1981; McSween and others, 1991).

On the basis of limited geochemical data, Horton and Izett (this volume, chap. E) suggest that the Langley Granite was emplaced in a volcanic arc setting, unlike chemically distinct granitoids of similar age within the Goochland terrane (fig. B11, table B6). Additional geochemical data are required for regional comparisons of the Langley Granite, the granite at Bayside, Va. (Horton, Aleinikoff, and others, 2002), and Neoproterozoic igneous rocks of similar age in the Carolina, Spring Hope, Roanoke Rapids, and Hatteras terranes (table B6).

Neoproterozoic igneous rocks are also found in Avalonian terranes of the northern Appalachians and Europe (summarized in Nance and Thompson, 1996) and in the Pan-African orogenic belts of West Africa (Dallmeyer and Villeneuve, 1987; Dallmeyer, 1989). The Langley Granite is similar in age to relatively undeformed intrusive rocks in New England, such as the Dedham, Milford, and Esmond Granites in Massachusetts and Rhode Island (Zartman and Naylor, 1984; Thompson and others, 1996), and to metavolcanic and metaplutonic rocks in Connecticut (Wintsch and Aleinikoff, 1987; Wintsch and others, 1992).

Preimpact target rocks of the Chesapeake Bay impact structure are considered to be a likely source for tektites of the North American strewn field (Poag and others, 1994; Koeberl and others, 1996, 2001; Glass, 2002). Furthermore, late Eocene tektites and microtektites from several sites in this field have Nd model ages of 620 to 670 Ma (Shaw and Wasserburg, 1982) and 630 Ma (Ngo and others, 1985), indicating that they were derived from Neoproterozoic source materials similar in age to, or slightly older than, the Langley Granite. The compositions of these tektites, including bediasites, georgiites, and microtektites, were summarized by Koeberl (1990) and Koeberl and others (2001).

Koeberl and others (2001) compared major-element, trace-element, and Nd and Sr isotopic compositions of some lower Tertiary sediments in the Chesapeake Bay target area with tektite compositions and found “no immediate similarity between the tektite compositions and the sediments” that they analyzed. We compared data for microtektites from Koeberl (1990, tables 1 and 2) with new data for the Langley Granite (table B2 and Horton and Izett, this volume, chap. E); the Langley Granite is similar in the major elements Si, Al, Fe, Mg, Ca, and K, is higher in Na and lower in Ti, but shows virtually no similarity in trace elements. Elements such as Na may be too volatile and mobile during melting for simple comparisons to be meaningful. More detailed chemical comparisons constrained by volumetric considerations and mass balance were not attempted at this stage because of the apparent dissimilarity in less mobile trace elements.

Tectonic Implications for Terranes beneath the Atlantic Coastal Plain

In the tectonic interpretation shown in figure B11, the USGS-NASA Langley corehole and the Chesapeake Bay impact structure are within the Chesapeake block. The southern margin of this block is shown as a suture, which was proposed by Lefort (1988, 1989) and Lefort and Max (1991) on the basis of geophysical data. They interpreted the Chesapeake block as the remnant of a tectonic indenter of Archean(?) African crust, left behind when the Atlantic Ocean opened. Similarities in age (table B6) between the Langley Granite and Neoproterozoic igneous rocks, including granites, in terranes to the south and southwest, raise doubts about the proposed suture. If the proposed suture (Lefort, 1989; Lefort and Max, 1991) is nonexistent, then the Roanoke Rapids and (or) Hatteras terrane may extend northward beneath the coastal plain into the target area of the impact structure (fig. B11). Testing these relations will require information on the age and character of host rocks that were intruded by the Langley Granite, new geochronology in the Roanoke Rapids and Hatteras terranes (where published dates in table B6 are too imprecise), and more geochemistry to support detailed chemical comparisons of igneous rocks in terranes beneath the coastal plain.

Table B6. Isotopic ages of selected Neoproterozoic igneous rocks for comparison with the age of the Langley Granite.

[Terranes are shown in figure B11]

Unit dated	Age (Ma)	Isotopic system and method	Reference*
Chesapeake block			
Langley Granite, Hampton, Va.....	612±10	²⁰⁶ Pb/ ²³⁸ U SHRIMP zircon	1, 5
Granite at Bayside, Va.....	625±11	²⁰⁶ Pb/ ²³⁸ U SHRIMP zircon	5
Carolina terrane			
Granite of Flat River complex, N.C.....	613.4+2.8/-2	U-Pb zircon, upper intercept	7
Diorite of Flat River complex, N.C.....	613.9+1.6/-1.5	U-Pb zircon, upper intercept	7
Osmond granite gneiss, N.C.....	612.4+5.2/-1.7	U-Pb zircon, upper intercept	7
Granodiorite near Clarkesville, Va.....	602±9	U-Pb zircon, upper intercept	4
Granite of Chapel Hill pluton, N.C.....	633+2/-1.5	U-Pb zircon, upper intercept	7
Felsic gneiss of Hyco Formation, N.C.....	619.9+4.5/-3	U-Pb zircon, upper intercept	7
Metarhyolite of Hyco Formation, N.C.....	615.7+3.7/-1.9	U-Pb zircon, upper intercept	7
Felsic metatuff of Hyco Formation, Va.....	621±8	U-Pb zircon, upper intercept	4
Felsic crystal metatuff of Hyco Formation, Va.....	616±4	U-Pb zircon, upper intercept	4
Spring Hope terrane			
Gneiss at Mill Creek, N.C.....	620±9	U-Pb zircon, upper intercept	2
Felsic crystal tuff near Spring Hope, N.C.....	590±3	U-Pb zircon, upper intercept	2
Roanoke Rapids terrane			
Metatonalite of Roanoke Rapids complex, N.C.....	668	²⁰⁷ Pb/ ²⁰⁶ Pb zircon, discordant	3
Metatonalite intruding(?) Easonburg Formation, N.C.....	607	²⁰⁷ Pb/ ²⁰⁶ Pb zircon, discordant	3
Hatteras terrane			
Amphibole quartz monzonite at Camp Lejeune, N.C.....	630±39	Rb/Sr whole rock	6
Garnet-cordierite-biotite granite at Stumpy Point, N.C.....	583±46	Rb/Sr whole rock	6
Goochland terrane			
Fine Creek Mills granite, Va. (A-type).....	629+4/-5	U-Pb zircon, lower intercept	8
Granite (SF98-2), Va. (A-type).....	630+9/-10	U-Pb zircon, lower intercept	8
Granite (SF99-11), Va. (A-type).....	600+7/-9	U-Pb zircon, lower intercept	8
Granite (SF99-20), Va. (A-type).....	588+9/-12	U-Pb zircon, lower intercept	8

*References: 1, this chapter; 2, Goldberg (1994); 3, Horton and Stern (1994); 4, Horton and others (1999); 5, Horton, Kunk, and others (2002); 6, Russell and others (1981); 7, Wortman and others (2000); 8, Owens and Tucker (2003).

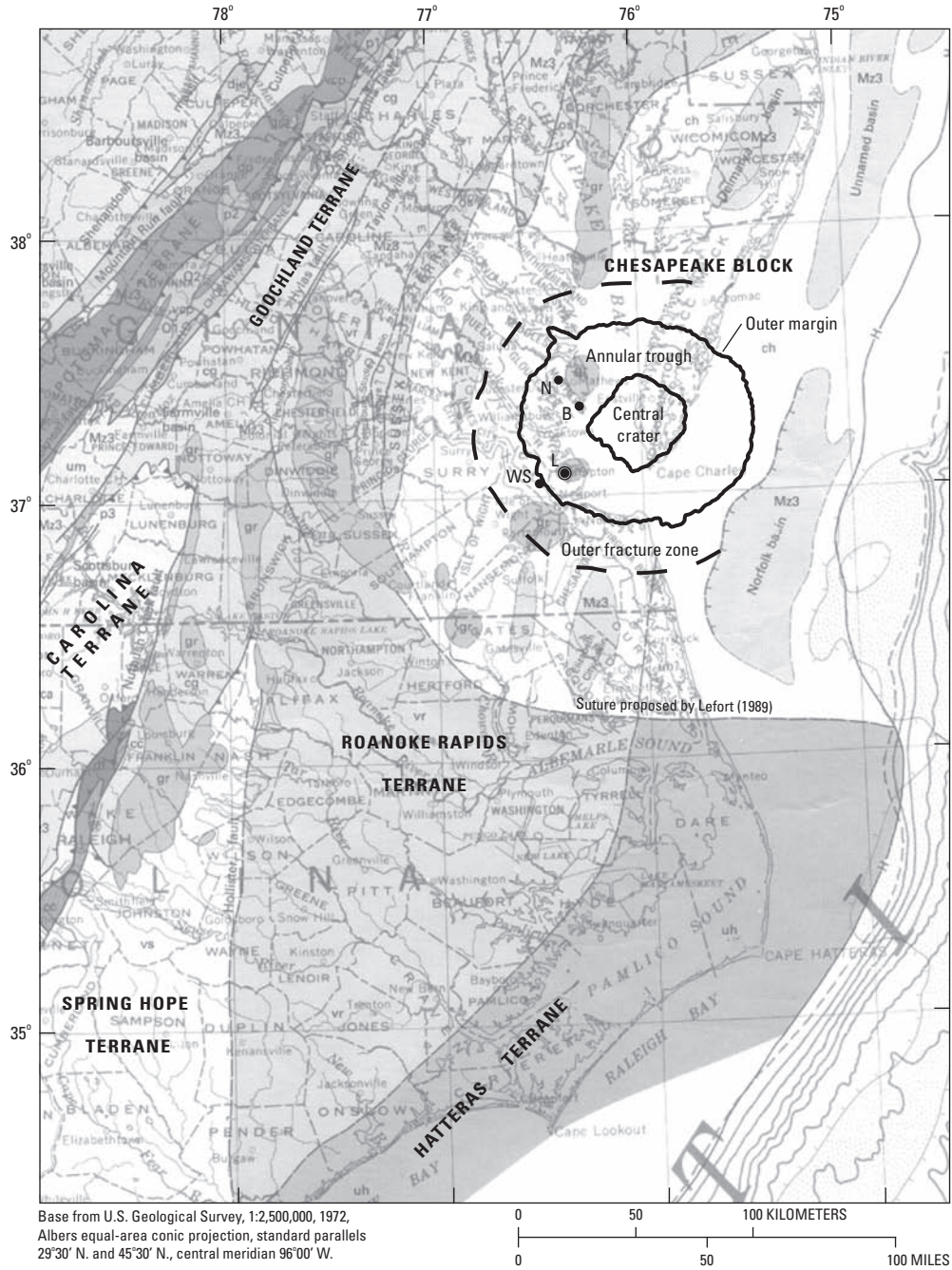


Figure B11. Map showing the location of the USGS-NASA Langley corehole (L), Hampton, Va., and the Chesapeake Bay impact structure in relation to a tectonostratigraphic terrane map (Horton and others, 1991) prepared before the structure was recognized. Other coreholes for this project are also shown: B, Bayside; N,

North; WS, Watkins School. Features of the impact structure are modified from Powars and Bruce (1999), Powars (2000), Johnson and others (2001), Powars, Johnson, and others (2002), and Edwards and Powars (2003).

If Mesoproterozoic Laurentian crust underlies the New Jersey Coastal Plain in the northern part of the Chesapeake block, as suggested by Rb/Sr geochronology (Sheridan and others, 1999), then an intervening suture is proposed here to separate those rocks from terrane(s) to the south that contain the Langley Granite and similar Neoproterozoic igneous rocks. However, that interpretation depends on a single Rb/Sr isochron age of 1.025 ± 0.036 Ga for metagabbro, hornblende, and quartzofeldspathic gneiss cuttings from a deep well at Cape May, N.J. (Sheridan and others, 1999); the geologic significance of a single isochron for such diverse rocks is questionable.

The age of the Langley Granite strongly suggests that coastal plain basement in the vicinity of the impact is related to peri-Gondwanan magmatic arc terranes such as the Carolina, Roanoke Rapids, and Avalon terranes, rather than Laurentia. Some peri-Gondwanan terranes, notably Avalon and Cadomia (not shown in fig. B11), have igneous rocks older than 650 Ma that have not yet been found in similar terranes of the southeastern United States (Secor and others, 1983; Samson and others, 1999; Wortman and others, 2000). Modern high-precision geochronology and geochemistry of exposed rocks in the Roanoke Rapids terrane are needed to determine whether rocks similar in age and composition to the Langley Granite and (or) rocks older than 650 Ma are present.

Lack of Discernible Impact-Related Deformation or Heating

No shock-metamorphosed minerals, shatter cones, or other features clearly attributable to the impact were seen in the Langley Granite in the Langley core, although crystalline-rock ejecta in the overlying impact-related sediments contain shock-metamorphosed quartz (Horton and others, 2001; Horton Aleinikoff, and others, 2002; Horton, Kunk, and others, 2002; Horton and Izett, this volume, chap. E). The argon and fission-track cooling ages of minerals show no discernible impact-related thermal disturbance in granite at this location near the outer margin of the impact structure. The apatite fission-track age of 184 ± 32 Ma is typical of cooling that followed the early Mesozoic rifting event throughout the region (Roden and Miller, 1991; Hulver, 1997; Naeser and others, 2001).

Seismic-reflection data suggest that impact-related faults penetrate crystalline basement beneath the coastal plain in the vicinity of the USGS-NASA Langley corehole (Catchings and others, this volume, chap. I). No such faults were documented in the core, but the chance of intersecting them was limited by having <9 m (<30 ft) of granite core.

Conclusions

The Langley Granite is peraluminous, nonfoliated, and highly chloritized. Fractures in the granite from the USGS-NASA Langley core are no more abundant than those in many

Piedmont cores, and most have lower greenschist-facies minerals suggesting that they predate the impact. The $^{206}\text{Pb}/^{238}\text{U}$ weighted average age of igneous zircon at 612 ± 10 Ma indicates a Neoproterozoic age for the granite. The $^{40}\text{Ar}/^{39}\text{Ar}$ ages of microcline and plagioclase may be related to regional cooling and uplift following the late Paleozoic Alleghanian orogeny. Apatite and zircon fission-track ages and apatite track lengths determined for sample NL2081 from the granite show no discernible impact-related thermal disturbance at this location about 19 km (12 mi) beyond the margin of the central crater. The granite has not yielded any shock-metamorphosed minerals or shatter cones or any evidence of an impact-related thermal event. Impact-generated faults were not detected in the granite core, although seismic-reflection data suggest that they penetrate coastal plain basement rocks in the general vicinity.

Acknowledgments

U.S. Geological Survey (USGS) investigations of the Chesapeake Bay impact structure are conducted in cooperation with the Hampton Roads Planning District Commission, the Virginia Department of Environmental Quality, and the National Aeronautics and Space Administration (NASA) Langley Research Center. The Hampton Roads Planning District Commission and the USGS provided funds for the drilling of the USGS-NASA Langley corehole. The NASA Langley Research Center provided extensive operational and logistical support for the drilling operation. The Virginia Department of Environmental Quality and the Department of Geology of the College of William and Mary provided extensive operational support at the drill site.

We thank Wendy Hodges (USGS) for mineral separations, Harvey Belkin (USGS) for assistance with the scanning-electron microscope, John Jackson (USGS) for assistance with the X-ray diffractometer, Glen A. Izett (College of William and Mary and USGS Emeritus) and Daniel J. Milton (USGS Emeritus) for consultations on shock-metamorphic criteria, and Yolanda Fong-Sam (USGS) for help in preparing figure B11. Reviews by Douglas W. Rankin (USGS) and Robert A. Ayuso (USGS) significantly improved the quality of this manuscript.

References Cited

- Aleinikoff, J.N., Zartman, R.E., Walter, Marianne, Rankin, D.W., Lyttle, P.T., and Burton, W.C., 1995, U-Pb ages of metarhyolites of the Catoctin and Mount Rogers Formations, central and southern Appalachians—Evidence for two pulses of Iapetan rifting: *American Journal of Science*, v. 295, no. 4, p. 428–454.
- Alexander, E.C., Jr., Mickelson, G.M., and Lanphere, M.A., 1978, MMhb-1; A new $^{40}\text{Ar}/^{39}\text{Ar}$ dating standard, *in* Zartman, R.E., ed., *Short papers of the Fourth International Conference, Geochronology, Cosmochronology, Isotope Geol-*

- ogy, 1978: U.S. Geological Survey Open-File Report 78–701, p. 6–8.
- Brandon, M.T., Roden-Tice, M.K., and Garver, J.I., 1998, Late Cenozoic exhumation of the Cascadia accretionary wedge in the Olympic Mountains, northwest Washington State: *Geological Society of America Bulletin*, v. 110, no. 8, p. 985–1009.
- Carpenter, B.S., and Reimer, G.M., 1974, Standard reference materials—Calibrated glass standards for fission track use: National Bureau of Standards Special Publication 260–49, 16 p.
- Catchings, R.D., Powars, D.S., Gohn, G.S., and Goldman, M.R., 2002, High-resolution seismic reflection survey of the southwestern margin of the Chesapeake Bay impact structure, Virginia [abs.]: *Eos, Transactions, American Geophysical Union*, v. 83, no. 19, spring meeting supplement of 7 May 2002, Abstract T21A–05, p. S352. (Also available online at <http://www.agu.org/meetings/waissm02.html>)
- Compston, W., Williams, I.S., and Meyer, C.E., 1984, U-Pb geochronology of zircons from lunar breccia 73217 using a sensitive high mass-resolution ion microprobe: *Journal of Geophysical Research*, v. 89B, suppl., p. 525–534.
- Dallmeyer, R.D., 1989, Contrasting accreted terranes in the southern Appalachian orogen and Atlantic-Gulf Coastal Plains and their correlations with West African sequences, *in* Dallmeyer, R.D., ed., *Terranes in the circum-Atlantic Paleozoic orogens*: Geological Society of America Special Paper 230, p. 247–267.
- Dallmeyer, R.D., and Villeneuve, Michael, 1987, $^{40}\text{Ar}/^{39}\text{Ar}$ mineral age record of polyphase tectonothermal evolution in the southern Mauritanide orogen, southeastern Senegal: *Geological Society of America Bulletin*, v. 98, no. 5, p. 602–611.
- Dalrymple, G.B., Alexander, E.C., Jr., Lanphere, M.A., and Kraker, G.P., 1981, Irradiation of samples for $^{40}\text{Ar}/^{39}\text{Ar}$ dating using the Geological Survey TRIGA reactor: U.S. Geological Survey Professional Paper 1176, 55 p.
- Daniels, D.L., and Leo, G.W., 1985, Geologic interpretation of basement rocks of the Atlantic Coastal Plain: U.S. Geological Survey Open-File Report 85–655, 45 p., 4 oversized pls.
- Denison, R.E., Raveling, H.P., and Rouse, J.T., 1967, Age and descriptions of subsurface basement rocks, Pamlico and Albemarle Sound areas, North Carolina: *American Association of Petroleum Geologists Bulletin*, v. 51, no. 2, p. 268–272.
- Dodson, M.H., 1979, Theory of cooling ages, *in* Jäger, E., and Hunziker, J.C., eds., *Lectures in isotope geology*: New York, Springer-Verlag, p. 194–202.
- Doyle, J.A., and Robbins, E.I., 1977, Angiosperm pollen zonation of the continental Cretaceous of the Atlantic Coastal Plain and its application to deep wells in the Salisbury embayment: *Palynology*, v. 1, p. 43–78.
- Edwards, L.E., and Powars, D.S., 2003, Impact damage to dinocysts from the late Eocene Chesapeake Bay event: *Palaios*, v. 18, no. 3, p. 275–285. (Also available online at <http://www.bioone.org/pdfserv/i0883-1351-018-03-0275.pdf>)
- Fetter, A.H., and Goldberg, S.A., 1995, Age and geochemical characteristics of bimodal magmatism in the Neoproterozoic Grandfather Mountain rift basin: *Journal of Geology*, v. 103, no. 3, p. 313–326.
- Fitzgerald, P.G., Sorkhabi, R.B., Redfield, T.F., and Stump, Edmund, 1995, Uplift and denudation of the central Alaska Range—A case study in the use of apatite fission track thermochronology to determine absolute uplift parameters: *Journal of Geophysical Research*, v. 100, no. B10, p. 20,175–20,191.
- Galbraith, R.F., 1981, On statistical models for fission track counts: *Mathematical Geology*, v. 13, no. 6, p. 471–478.
- Gallagher, Kerry, 1995, Evolving temperature histories from apatite fission-track data: *Earth and Planetary Science Letters*, v. 136, no. 3–4, p. 421–435.
- Garihan, J.M., Preddy, M.S., and Ranson, W.A., 1993, Summary of mid-Mesozoic brittle faulting in the Inner Piedmont and nearby Charlotte belt of the Carolinas, *in* Hatcher, R.D., Jr., and Davis, T.L., eds., *Studies of Inner Piedmont geology with a focus on the Columbus promontory—Carolina Geological Society annual field trip, November 6–7, 1993*: Carolina Geological Society, p. 55–65.
- Glass, B.P., 2002, Distal impact ejecta from the Chesapeake Bay impact structure [abs.]: *Geological Society of America Abstracts with Programs*, v. 34, no. 6, p. 466.
- Gleadow, A.J.W., Duddy, I.R., Green, P.F., and Lovering, J.F., 1986, Confined fission track lengths in apatite—A diagnostic tool for thermal history analysis: *Contributions to Mineralogy and Petrology*, v. 94, no. 4, p. 405–415.
- Gleadow, A.J.W., Hurford, A.J., and Quaife, R.D., 1976, Fission track dating of zircon—Improved etching techniques: *Earth and Planetary Science Letters*, v. 33, no. 2, p. 273–276.
- Glover, Lynn, III, Sheridan, R.E., Holbrook, W.S., Ewing, John, Talwani, Manik, Hawman, R.B., and Wang, Ping, 1997, Paleozoic collisions, Mesozoic rifting and structure of the Middle Atlantic States continental margin; An “EDGE” Project report, *in* Glover, Lynn, III, and Gates, A.E., eds., *Central and southern Appalachian sutures—Results of the EDGE Project and related studies*: Geological Society of America Special Paper 314, p. 107–135.
- Gohn, G.S., Clark, A.C., Queen, D.G., Levine, J.S., McFarland, E.R., and Powars, D.S., 2001, Operational summary for the USGS-NASA Langley corehole, Hampton, Virginia: U.S. Geological Survey Open-File Report 01–87–A, 21 p., available online at <http://pubs.usgs.gov/of/2001/of01-087/>
- Gohn, G.S., Powars, D.S., Bruce, T.S., Self-Trail, J.M., Weems, R.E., Edwards, L.E., Horton, J.W., Jr., Izett, G.A., and Johnson, G.H., 2001, Preliminary interpretation of the USGS-NASA Langley corehole, Chesapeake Bay impact structure, York-James Peninsula, Hampton, VA [abs.]: *Geological Society of America Abstracts with Programs*, v. 33, no. 2, p. A–24.
- Goldberg, S.A., 1994, U-Pb geochronology of volcanogenic terranes of the eastern North Carolina Piedmont—Preliminary results, *in* Stoddard, E.F., and Blake, D.E., eds., *Geology and field trip guide, western flank of the Raleigh meta-*

- morphic belt, North Carolina—Carolina Geological Society field trip guidebook, November 5–6, 1994: Raleigh, N.C., North Carolina Geological Society, p. 13–17. (Also available online at <http://carolinageologicalsociety.org/gb%201994.pdf>)
- Green, P.F., Duddy, I.R., Gleadow, A.J.W., and Lovering, J.F., 1989, Apatite fission-track analysis as a paleotemperature indicator for hydrocarbon exploration, *in* Naeser, N.D., and McCulloh, T.H., eds., *Thermal history of sedimentary basins—Methods and case histories*: New York, Springer-Verlag, p. 181–195.
- Haugerud, R.A., and Kunk, M.J., 1988, ArAr*, a computer program for reduction of ^{40}Ar - ^{39}Ar data: U.S. Geological Survey Open-File Report 88–261, 68 p.
- Horton, J.W., Jr., Aleinikoff, J.N., Burton, W.C., Peper, J.D., and Hackley, P.C., 1999, Geologic framework of the Carolina slate belt in southern Virginia—Insights from geologic mapping and U-Pb geochronology [abs.]: Geological Society of America Abstracts with Programs, v. 31, no. 7, p. A–476.
- Horton, J.W., Jr., Aleinikoff, J.N., Izett, G.A., Naeser, C.W., and Naeser, N.D., 2001, Crystalline rocks from the first core-hole to basement in the Chesapeake Bay impact structure, Hampton, Virginia [abs.]: Geological Society of America Abstracts with Programs, v. 33, no. 6, p. A–448.
- Horton, J.W., Jr., Aleinikoff, J.N., Izett, G.A., Naeser, N.D., Naeser, C.W., and Kunk, M.J., 2002, Crystalline basement and impact-derived clasts from three coreholes in the Chesapeake Bay impact structure, southeastern Virginia [abs.]: Eos, Transactions, American Geophysical Union, v. 83, no. 19, spring meeting supplement of 7 May 2002, Abstract T21A–03, p. S351. (Also available online at <http://www.agu.org/meetings/waissm02.html>)
- Horton, J.W., Jr., Drake, A.A., Jr., Rankin, D.W., and Dallmeyer, R.D., 1991, Preliminary tectonostratigraphic terrane map of the central and southern Appalachians: U.S. Geological Survey Miscellaneous Investigations Series Map I–2163, scale 1:2,000,000.
- Horton, J.W., Jr., Kunk, M.J., Naeser, C.W., Naeser, N.D., Aleinikoff, J.N., and Izett, G.A., 2002, Petrography, geochronology, and significance of crystalline basement rocks and impact-derived clasts in the Chesapeake Bay impact structure, southeastern Virginia [abs.]: Geological Society of America Abstracts with Programs, v. 34, no. 6, p. 466.
- Horton, J.W., Jr., and Stern, T.W., 1994, Tectonic significance of preliminary uranium-lead ages from the eastern Piedmont of North Carolina [abs.]: Geological Society of America Abstracts with Programs, v. 26, no. 4, p. 21.
- Hulver, M.L., 1997, Post-orogenic evolution of the Appalachian Mountain system and its foreland: Chicago, University of Chicago, Ph.D. dissertation, 1,055 p.
- Hurfurd, A.J., and Green, P.F., 1982, A users' guide to fission track dating calibration: *Earth and Planetary Science Letters*, v. 59, no. 2, p. 343–354.
- Hurfurd, A.J., and Green, P.F., 1983, The zeta age calibration of fission-track dating: *Isotope Geoscience*, v. 1, p. 285–317.
- Johnson, G.H., Powars, D.S., Bruce, T.S., Beach, T.A., Harris, M.S., and Goodwin, B.K., 2001, Post-impact effects of the Eocene Chesapeake Bay impact, lower York-James Peninsula, Virginia: Virginia Geological Field Conference, 31st, Williamsburg, Virginia, October 19 and 20, 2001 [Guidebook], 40 p.
- Johnson, S.S., 1975, Bouguer gravity in southeastern Virginia: Virginia Division of Mineral Resources Report of Investigations 39, 42 p.
- Koeberl, Christian, 1990, The geochemistry of tektites—An overview: *Tectonophysics*, v. 171, no. 1–4, p. 405–422.
- Koeberl, Christian, Kruger, F.J., and Poag, C.W., 2001, Geochemistry of surficial sediments near the Chesapeake Bay impact structure and the search for source rocks of the North American tektites [abs.]: Lunar and Planetary Science Conference, 32d, Houston, Tex., March 12–16, 2001, Abstract 1333, available online at <http://www.lpi.usra.edu/meetings/lpsc2001/pdf/1333.pdf>
- Koeberl, Christian, Poag, C.W., Reimold, W.U., and Brandt, Dion, 1996, Impact origin of the Chesapeake Bay structure and the source of the North American tektites: *Science*, v. 271, no. 5253, p. 1263–1266.
- Kohn, B.P., Wagner, M.E., Lutz, T.M., and Organist, G., 1993, Anomalous Mesozoic thermal regime, central Appalachian Piedmont—Evidence from sphene and zircon fission-track dating: *Journal of Geology*, v. 101, no. 6, p. 779–794.
- Laslett, G.M., Green, P.F., Duddy, I.R., and Gleadow, A.J.W., 1987, Thermal annealing of fission tracks in apatite—2. A quantitative analysis: *Chemical Geology (Isotope Geoscience Section)*, v. 65, no. 1, p. 1–13.
- Laslett, G.M., Kendall, W.S., Gleadow, A.J.W., and Duddy, I.R., 1982, Bias in measurement of fission-track length distributions: *Nuclear Tracks and Radiation Measurements*, v. 6, no. 2–3, p. 79–85.
- Lefort, J.P., 1988, Imprint of the Reguibat uplift (Mauritania) onto the central and southern Appalachians of the U.S.A.: *Journal of African Earth Sciences*, v. 7, no. 2, p. 433–442.
- Lefort, J.P., 1989, Basement correlation across the North Atlantic: Berlin, Springer-Verlag, 148 p.
- Lefort, J.P., and Max, M.D., 1991, Is there an Archean crust beneath Chesapeake Bay?: *Tectonics*, v. 10, no. 1, p. 213–226.
- LeVan, D.C., and Pharr, R.F., 1963, A magnetic survey of the coastal plain in Virginia: Virginia Division of Mineral Resources Report of Investigations 4, 17 p., 3 oversized pls.
- Mann, V.I., Clarke, T.G., Hayes, L.D., and Kirstin, D.S., 1965, Geology of the Chapel Hill quadrangle, North Carolina: Raleigh, North Carolina Division of Mineral Resources Special Publication 1, 35 p., 1 oversized pl.
- McDougall, Ian, and Harrison, T.M., 1999, Geochronology and thermochronology by the $^{40}\text{Ar}/^{39}\text{Ar}$ method, (2d ed.): New York, Oxford University Press, 269 p.
- McGee, V.E., Johnson, N.M., and Naeser, C.W., 1985, Simulated fissioning of uranium and testing of the fission-track dating method: *Nuclear Tracks and Radiation Measurements*, v. 10, no. 3, p. 365–379.

- McSween, H.Y., Jr., Speer, J.A., and Fullagar, P.D., 1991, Plutonic rocks, *in* Horton, J.W., Jr., and Zullo, V.A., eds., *The geology of the Carolinas*, Carolina Geological Society fiftieth anniversary volume: Knoxville, University of Tennessee Press, p. 109–126.
- Naeser, C.W., 1976, Fission track dating: U.S. Geological Survey Open-File Report 76–190, 58 p.
- Naeser, C.W., 1979, Fission-track dating and geologic annealing of fission tracks, *in* Jäger, E., and Hunziker, J.C., eds., *Lectures in isotope geology*: New York, Springer-Verlag, p. 154–169.
- Naeser, C.W., Naeser, N.D., Kunk, M.J., Morgan, B.A., III, Schultz, A.P., Southworth, C.S., and Weems, R.E., 2001, Paleozoic through Cenozoic uplift, erosion, stream capture, and depositional history in the Valley and Ridge, Blue Ridge, Piedmont, and Coastal Plain provinces of Tennessee, North Carolina, Virginia, Maryland, and District of Columbia [abs.]: *Geological Society of America Abstracts with Programs*, v. 33, no. 6, p. A312.
- Naeser, N.D., Naeser, C.W., and McCulloh, T.H., 1989, The application of fission-track dating to the depositional and thermal history of rocks in sedimentary basins, *in* Naeser, N.D., and McCulloh, T.H., eds., *Thermal history of sedimentary basins—Methods and case histories*: New York, Springer-Verlag, p. 157–180.
- Nance, R.D., and Thompson, M.D., 1996, Avalonian and related peri-Gondwanan terranes of the circum-North Atlantic—An introduction, *in* Nance, R.D., and Thompson, M.D., eds., *Avalonian and related peri-Gondwanan terranes of the circum-North Atlantic*: Geological Society of America Special Paper 304, p. 1–7.
- Ngo, H.H., Wasserburg, G.J., and Glass, B.P., 1985, Nd and Sr isotopic compositions of tektite material from Barbados and their relationship to North American tektites: *Geochimica et Cosmochimica Acta*, v. 49, no. 6, p. 1479–1485.
- Owens, B.E., and Tucker, R.D., 2003, Geochronology of the Mesoproterozoic State Farm Gneiss and associated Neoproterozoic granitoids, Goochland terrane, Virginia: *Geological Society of America Bulletin*, v. 115, no. 8, p. 972–982.
- Poag, C.W., 1996, Structural outer rim of Chesapeake Bay impact crater—Seismic and bore hole evidence: *Meteoritics & Planetary Science*, v. 31, no. 2, p. 218–226.
- Poag, C.W., 1997, The Chesapeake Bay bolide impact; A convulsive event in Atlantic Coastal Plain evolution: *Sedimentary Geology*, v. 108, no. 1–4, p. 45–90.
- Poag, C.W., 1999, Chesapeake invader; Discovering America's giant meteorite crater: Princeton, N.J., Princeton University Press, 183 p.
- Poag, C.W., 2002, Structure and morphology of the Chesapeake Bay submarine impact crater [abs.]: *Geological Society of America Abstracts with Programs*, v. 34, no. 6, p. 465.
- Poag, C.W., and the Chesapeake Coring Team, 2001, Drilling to basement inside the Chesapeake Bay crater [abs.]: *Lunar and Planetary Science Conference*, 32d, Houston, Tex., March 12–16, 2001, Abstract 1203, available online at <http://www.lpi.usra.edu/meetings/lpsc2001/pdf/1203.pdf>
- Poag, C.W., Hutchinson, D.R., Colman, S.M., and Lee, M.W., 1999, Seismic expression of the Chesapeake Bay impact crater; Structural and morphologic refinements based on new seismic data, *in* Dressler, B.O., and Sharpton, V.L., eds., *Large meteorite impacts and planetary evolution; II: Geological Society of America Special Paper 339*, p. 149–164.
- Poag, C.W., Plescia, J.B., and Molzer, P.C., 1999, Chesapeake Bay impact structure; Geology and geophysics [abs.], *in* Gersonde, Rainer, and Deutsch, Alexander, eds., *Oceanic impacts; Mechanisms and environmental perturbations; ESF-IMPACT Workshop, April 15–April 17, 1999*, Alfred Wegener Institute for Polar and Marine Research, Bremerhaven, Germany, *Abstracts: Berichte zur Polarforschung (Reports on Polar Research)*, v. 343, p. 79–83.
- Poag, C.W., Powars, D.S., Poppe, L.J., and Mixon, R.B., 1994, Meteoroid mayhem in Ole Virginny—Source of the North American tektite strewn field: *Geology*, v. 22, no. 8, p. 691–694.
- Poag, C.W., Powars, D.S., Poppe, L.J., Mixon, R.B., Edwards, L.E., Folger, D.W., and Bruce, Scott, 1992, Deep Sea Drilling Project Site 612 bolide event—New evidence of a late Eocene impact-wave deposit and a possible impact site, *U.S. East Coast: Geology*, v. 20, no. 9, p. 771–774.
- Powars, D.S., 2000, The effects of the Chesapeake Bay impact crater on the geologic framework and the correlation of hydrogeologic units of southeastern Virginia, south of the James River: *U.S. Geological Survey Professional Paper 1622*, 53 p., 1 oversize pl. (Also available online at <http://pubs.usgs.gov/prof/p1622>)
- Powars, D.S., and Bruce, T.S., 1999, The effects of the Chesapeake Bay impact crater on the geological framework and correlation of hydrogeologic units of the lower York-James Peninsula, Virginia: *U.S. Geological Survey Professional Paper 1612*, 82 p., 9 oversize pls. (Also available online at <http://pubs.usgs.gov/prof/p1612/>)
- Powars, D.S., Bruce, T.S., Bybell, L.M., Cronin, T.M., Edwards, L.E., Frederiksen, N.O., Gohn, G.S., Horton, J.W., Jr., Izett, G.A., Johnson, G.H., Levine, J.S., McFarland, E.R., Poag, C.W., Quick, J.E., Schindler, J.S., Self-Trail, J.M., Smith, M.J., Stamm, R.G., and Weems, R.E., 2001, Preliminary geologic summary for the USGS-NASA Langley corehole, Hampton, Virginia: *U.S. Geological Survey Open-File Report 01–87–B*, 20 p., available online at <http://pubs.usgs.gov/of/2001/of01-087/>
- Powars, D.S., Gohn, G.S., Edwards, L.E., Catchings, R.D., Bruce, T.S., Johnson, G.H., and Poag, C.W., 2002, Lithostratigraphic framework of the crater-fill deposits; Western annular trough, Chesapeake Bay impact crater [abs.]: *Geological Society of America Abstracts with Programs*, v. 34, no. 6, p. 465.
- Powars, D.S., Johnson, G.H., Edwards, L.E., Horton, J.W., Jr., Gohn, G.S., Catchings, R.D., McFarland, E.R., Izett, G.A.,

- Bruce, T.S., Levine, J.S., and Pierce, H.A., 2002, An expanded Chesapeake Bay impact structure; eastern Virginia: New corehole and geophysical data [abs.]: Lunar and Planetary Science Conference, 33d, League City, Tex., March 11–15, 2002, Abstract 1034, available online at <http://www.lpi.usra.edu/meetings/lpsc2002/pdf/1034.pdf>
- Powars, D.S., Mixon, R.B., and Bruce, Scott, 1992, Uppermost Mesozoic and Cenozoic geologic cross section, outer coastal plain of Virginia, in Gohn, G.S., ed., Proceedings of the 1988 U.S. Geological Survey Workshop on the Geology and Hydrology of the Atlantic Coastal Plain: U.S. Geological Survey Circular 1059, p. 85–101.
- Pratt, T.L., Coruh, Cohit, Costain, J.K., and Glover, Lynn, III, 1988, A geophysical study of the Earth's crust in central Virginia; Implications for Appalachian crustal structure: *Journal of Geophysical Research*, v. 93, no. B6, p. 6649–6674.
- Rankin, D.W., 1994, Continental margin of the eastern United States; Past and present, in Speed, R.C., ed., Phanerozoic evolution of North American continent-ocean transitions—The Decade of North American Geology summary volume to accompany the DNAG continent-ocean transect series: Boulder, Colo., Geological Society of America, p. 129–218.
- Reimold, W.U., Koeberl, Christian, and Poag, C.W., 2002, Chesapeake Bay impact crater; Petrographic and geochemical investigations of the impact breccia fill [abs.]: Geological Society of America Abstracts with Programs, v. 34, no. 6, p. 466.
- Reinhardt, Juergen, Christopher, R.A., and Owens, J.P., 1980, Lower Cretaceous stratigraphy of the core, in *Geology of the Oak Grove core: Virginia Division of Mineral Resources Publication 20*, pt. 1, p. 31–52, 1 pl.
- Roddick, J.C., 1983, High precision intercalibration of ^{40}Ar - ^{39}Ar standards: *Geochimica et Cosmochimica Acta*, v. 47, no. 5, p. 887–898.
- Roden, M.K., and Miller, D.S., 1991, Tectono-thermal history of Hartford, Deerfield, Newark, and Taylorsville Basins, eastern United States, using fission-track analysis: *Schweizerische Mineralogische und Petrographische Mitteilungen*, v. 71, p. 187–203.
- Russell, G.S., Russell, C.W., Speer, J.A., and Glover, Lynn, III, 1981, Rb-Sr evidence of latest Precambrian to Cambrian and Alleghanian plutonism along the eastern margin of the sub-coastal plain Appalachians, North Carolina and Virginia [abs.]: Geological Society of America Abstracts with Programs, v. 13, no. 7, p. 543.
- Russell, G.S., Speer, J.A., and Russell, C.W., 1985, The Portsmouth Granite, a 263 Ma postmetamorphic biotite granite beneath the Atlantic Coastal Plain, Suffolk, Virginia: *Southeastern Geology*, v. 26, no. 2, p. 81–93.
- Samson, S.D., Secor, D.T., and Stern, R., 1999, Provenance and paleogeography of Neoproterozoic circum-Atlantic arc-terrane—Constraints from U-Pb ages of detrital zircons [abs.]: Geological Society of America Abstracts with Programs, v. 31, no. 7, p. 429.
- Secor, D.T., Jr., Samson, S.L., Snoke, A.W., and Palmer, A.R., 1983, Confirmation of the Carolina slate belt as an exotic terrane: *Science*, v. 221, no. 4611, p. 649–651.
- Shaw, H.F., and Wasserburg, G.J., 1982, Age and provenance of the target materials for tektites and possible impactites as inferred from Sm-Nd and Rb-Sr systematics: *Earth and Planetary Science Letters*, v. 60, no. 2, p. 155–177.
- Sheridan, R.E., Maguire, T.J., Feigenson, M.D., Patino, L.C., and Volkert, R.A., 1999, Grenville age of basement rocks in Cape May, N.J. well—New evidence for Laurentian crust in U.S. Atlantic Coastal Plain basement Chesapeake terrane: *Journal of Geodynamics*, v. 27, no. 4–5, p. 623–633.
- Speer, J.A., 1981, Petrology of cordierite- and almandine-bearing granitoid plutons of the southern Appalachian Piedmont, U.S.A.: *Canadian Mineralogist*, v. 19, pt. 1, p. 35–46.
- Stacey, J.S., and Kramers, J.D., 1975, Approximation of terrestrial lead isotope evolution by a two-stage model: *Earth and Planetary Science Letters*, v. 26, no. 2, p. 207–221.
- Steiger, R.H., and Jäger, E., comps., 1977, Subcommittee on geochronology—Convention on the use of decay constants in geo- and cosmochronology: *Earth and Planetary Science Letters*, v. 36, no. 3, p. 359–362.
- Streckeisen, A.L., chairman, 1973, Plutonic rocks—Classification and nomenclature recommended by the IUGS Subcommittee on the Systematics of Igneous Rocks: *Geotimes*, v. 18, no. 10, p. 26–30.
- Streckeisen, A.L., 1976, To each plutonic rock its proper name: *Earth-Science Reviews*, v. 12, no. 1, p. 1–33.
- Su, Qi, Goldberg, S.A., and Fullagar, P.D., 1994, Precise U-Pb zircon ages of Neoproterozoic plutons in the southern Appalachian Blue Ridge and their implications for the initial rifting of Laurentia: *Precambrian Research*, v. 68, no. 1–2, p. 81–95.
- Thompson, M.D., Hermes, O.D., Bowring, S.A., Isachsen, C.E., Besancon, J.R., and Kelly, K.L., 1996, Tectonostratigraphic implications of late Proterozoic U-Pb zircon ages in the Avalon Zone of southeastern New England, in Nance, R.D., and Thompson, M.D., eds., *Avalonian and related peri-Gondwanan terranes of the circum-North Atlantic: Geological Society of America Special Paper 304*, p. 179–191.
- United States Geological Survey, 1986, [Topographic map of the] Newport News North, Virginia [7.5-minute quadrangle showing photorevisions of the 1965 map]: Reston, Va., U.S. Geological Survey, scale 1:24,000.
- Williams, I.S., and Claesson, S., 1987, Isotopic evidence for the Precambrian provenance and Caledonian metamorphism of high grade paragneisses from the Seve Nappes, Scandinavian Caledonides, II. Ion microprobe zircon U-Th-Pb: *Contributions to Mineralogy and Petrology*, v. 97, no. 2, p. 205–217.
- Wintsch, R.P., and Aleinikoff, J.N., 1987, U-Pb isotopic and geologic evidence for late Paleozoic anatexis, deformation, and accretion of the late Proterozoic Avalon terrane, south-

B28 Studies of the Chesapeake Bay Impact Structure—The USGS-NASA Langley Corehole, Hampton, Va.

- central Connecticut: *American Journal of Science*, v. 287, no. 2, p. 107–126.
- Wintsch, R.P., Sutter, J.F., Kunk, M.J., Aleinikoff, J.N., and Dorais, M.J., 1992, Contrasting P-T-t paths—Thermochronologic evidence for a late Paleozoic final assembly of the Avalon composite terrane in the New England Appalachians: *Tectonics*, v. 11, no. 3, p. 672–689.
- Wortman, G.L., Samson, S.D., and Hibbard, J.P., 2000, Precise U-Pb zircon constraints on the earliest magmatic history of the Carolina terrane: *Journal of Geology*, v. 108, no. 3, p. 321–338.
- York, D., 1969, Least squares fitting of a straight line with correlated errors: *Earth and Planetary Science Letters*, v. 5, no. 5, p. 320–324.
- Zartman, R.E., and Naylor, R.S., 1984, Structural implications of some radiometric ages of igneous rocks in southeastern New England: *Geological Society of America Bulletin*, v. 95, no. 5, p. 522–539.

Appendix B1. Descriptions of Samples from the Langley Granite in the USGS-NASA Langley Core

Samples from the USGS-NASA Langley core that are described in this chapter were taken from core box 206 (fig. B3A). Samples are identified by the letters NL followed by a number indicating depth in feet. Parts of the core shown in figure B4C,E,F,G were not sampled for analysis.

The thin sections were studied by Horton and also were examined by Glen A. Izett (College of William and Mary and USGS Emeritus) and Daniel J. Milton (USGS Emeritus). These examinations revealed no shock-metamorphic features.

Sample NL2080.1

[2 thin sections (fig. B4D)]

Depth.—634.01 m (2,080.1 ft); core box 206.

Description.—Sample NL2080.1 consists of granite from the extreme upper end of the interval contained in sample NL2081 (described below). The granite is massive, pale red, medium grained, and nonfoliated; albite and chlorite fill fractures and faults. The fabric is seriate-inequigranular, hypidiomorphic, and isotropic. Mineral percentages are in table B1.

Sample NL2081

Depth.—In sawed half of the drill core from 633.98 to 634.81 m (2,080.0 to 2,082.7 ft) depth; core box 206.

Description.—Sample NL2081 consists of granite that is massive, pale red, medium grained, and nonfoliated. About 2 kilograms (about 4.4 pounds) of granite was processed for mineral separates of zircon (fig. B5) for SHRIMP U-Pb geochronology (fig. B6, table B3), microcline and plagioclase for $^{40}\text{Ar}/^{39}\text{Ar}$ geochronology (fig. B7, table B4), and zircon and apatite for fission-track geochronology (table B5). The presence of clinocllore, quartz, titanite, hematite, and clinozoisite was confirmed by X-ray diffraction of a mineral separate having a specific gravity between 3.17 and 3.32. NL2080.1 thin sections are from the extreme upper end of the interval contained in this larger sample. Data from NL2080.1 served as a guide for collecting this larger geochronology sample, which encompasses and extends beyond it.

Sample NL2083

Depth.—634.81 to 634.93 m (2,082.7 to 2,083.1 ft); core box 206.

Description.—White albite coating a single joint surface from 634.81 to 634.93 m (2,082.7 to 2,083.1 ft) depth in the granite core. The albite was confirmed by X-ray diffraction and dated by the $^{40}\text{Ar}/^{39}\text{Ar}$ age-spectrum method (fig. B7, table B4). NL2083.1 thin sections, which do not include the joint, are from rock adjacent to the lower end of this sample.

Sample NL2083.1

[2 thin sections (fig. B4A,B)]

Depth.—634.93 m (2,083.1 ft); core box 206.

Description.—Sample NL2083.1 consists of granite from just below the lower end of sample NL2083 (described above). The granite is massive, pale red, medium grained, and nonfoliated. The fabric is seriate-inequigranular, hypidiomorphic, and isotropic. Mineral percentages are in table B1, and chemical composition is in table B2.

Gray minerals were separated by color from part of the same rock sample; the gray minerals were determined by X-ray diffraction to be quartz, albite, and microcline. Semi-quantitative mineral compositions based on scanning-electron microscopy (SEM) follow:

- K-feldspar—66.6 percent SiO_2 , 18.7 percent Al_2O_3 , 13.2 percent K_2O , 1.5 percent Na_2O
- Albite—65.5 percent SiO_2 , 20.6 percent Al_2O_3 , 12.7 percent Na_2O , 0.5 percent CaO , 0.3 percent K_2O
- Oligoclase—66.5 percent SiO_2 , 21.5 percent Al_2O_3 , 10.4 percent Na_2O , 1.5 percent CaO
- Chlorite—Mg much more abundant than Fe

Accessory and trace minerals confirmed by SEM are titanite, zircon, apatite, thorite (intergrown with zircon), a titanium oxide, and monazite as minute inclusions in iron-titanium oxide; inclusions in chlorite were identified as albite, an epidote mineral, titanite, and Fe oxide having a very low Ti content.